# DWR4 with ACM

Datawell - Oceanographic Instruments

**The in-home developed, Directional Waverider that integrates wave and current measurements has been launched.**

**DWR Wave measurements: same sensor, new data processing**

The wave sensor of the Directional Waverider equipped with the Acoustic Current Meter option (DWR4/ACM for short) is identical to the sensor in the well-known Directional Waverider MkI, II and III. Processing of the measured data is now performed at the doubled sample frequency of 2.56 Hz. The high frequency limit of the heave and direction signals is shifted from 0.58 to 1.0 Hz. With this choice, the high frequency limit of the wave buoy is determined by the hydrodynamic response of the hull, not by the onboard instrumentation.

In addition, the DWR4 transmission protocol allows for a superior heave and horizontal displacement resolution. Easy comparison of the new DWR4 output to the familiar DWR-MkIII results is facilitated in the accompanying waves4 software suite.

**Operational improvements**

Extra features of the DWR4 compared to the DWR-MkIII to facilitate operation are:

- For identification, the buoy is tagged with an electronic ID-number (or actually two ID's for hull and hatch cover separately) which is transmitted along the measured data.
- As a kind of health parameters, the temperature of the Hippy-40 sensor as well as that of the hatch cover electronics are measured.
- For better energy management, the energy used from the batteries and the energy supplied by the optional solar panel are measured.

An operational difference between the DWR-MkIII and the DWR4 is the criterion for the flashlight. This has changed from light detection to a sunset/sunrise algorithm based on the GPS position and time.



Datawell BV
Zomerluststraat 4
2012 LM Haarlem
The Netherlands

T +31 72 534 52 98
F +31 72 572 64 06
E sales@datawell.nl
W www.datawell.nl

# DWR4 with ACM

Datawell - Oceanographic Instruments

**The Acoustic Current Meter**

The DWR4 is extended with a surface current meter. This Acoustic Current Meter, or ACM for short, combines a robust measuring principle, Doppler shift, with a mechanical design that avoids vulnerability. This results in a coherent oceanographic instrument

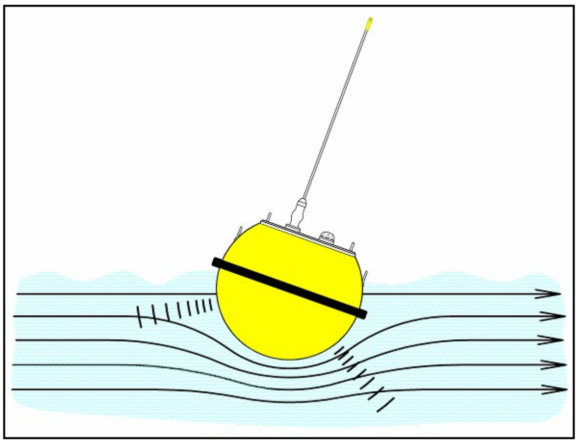

that meets the challenges at sea.

By integrating three acoustic transducers in the hull of the well-known Directional Waverider, the surface water velocity can be measured. The current is determined at roughly one metre below sea level, by measuring the Doppler shift of reflected 2 MHz pings. This robust and reliable method accords well with the Hippy 40 wave sensor, the standard in wave direction measurements.

Every 10 minutes, the magnitude and direction of the surface current are measured by three acoustic transducers. The transducers all face 30° down and are 120° laterally apart. Each transducer measures the projection of the current velocity along its axis.

By time-gating the sensitive distance for the water velocity measurement is between 0.5 and 1.75 m from the hull. The current flow is affected by the presence of the Directional Waverider; close to the hull, the radial component of the velocity will be small, as opposed to the tangential components. Potential theory predicts thus an underestimation of a few percent. No compensation for this effect is applied.

The velocities as measured by the transducers are converted into a North-West-Vertical water velocity by means of the pitch-roll sensor and the compass of the DWR.

During one minute each transducer fires 150 acoustic pings. The velocity measurements are quality-controlled and averaged.

**Impact of waves on the current measurement**

Due to the orbital nature of the wave motion, the horizontal velocity is not a constant over time and place. Different ranges of wave periods have a different impact on the water velocity measurement. Short waves, up to 1 second (1.5 m wavelength) average out in the volume over which the velocity is measured. Due to the size of the DWR, the wavelength is too small to make the buoy follow the waves and introduce artificial water velocity.

Waves which have a period smaller than 30 seconds (wavelength smaller than 1.5 km), can affect the velocity measured by the individual pings. Being moored flexibly, the Waverider buoy is able to follow the wave motion, which reduces the impact by the horizontal wave velocity significantly.

Wave periods beyond 30 seconds (wavelength longer than 1.5 km) will affect the individual water velocity measurement in the case of a moored buoy.

**Impact of tidal motion on the current measurement**

At the change of tide, the direction of the current typically changes by some 180° and the buoy traverses from one stationary position to the other. During the crossing, the actual water velocity is the vector-sum of the current as measured by the buoy plus the velocity of the buoy itself. The velocity of the buoy when moving from one location to the other is typically small, up to a couple of centimetres per second, depending on the location and the mooring line length. At some locations however, the buoy velocity can be one or more decimetres per second at every change of tide.

By measuring the position of the buoy by means of GPS every 2 minutes the buoy velocity is obtained. Each GPS-location is validated and results in a calculated buoy velocity that is transmitted alongside the velocity by the acoustic transducers.

**Operational performance**

During the development of the ACM option, several field tests have been performed off the coast near IJmuiden, The Netherlands, where a pole mounted ADCP provided reference data. Significant wave height during the test period rose to 4.5 m. Water velocity oscillated with the tides between 1 m/s to the south and 1 m/s to the north. Agreement with the ADCP is typically within 2 % and 0.02 m/s.

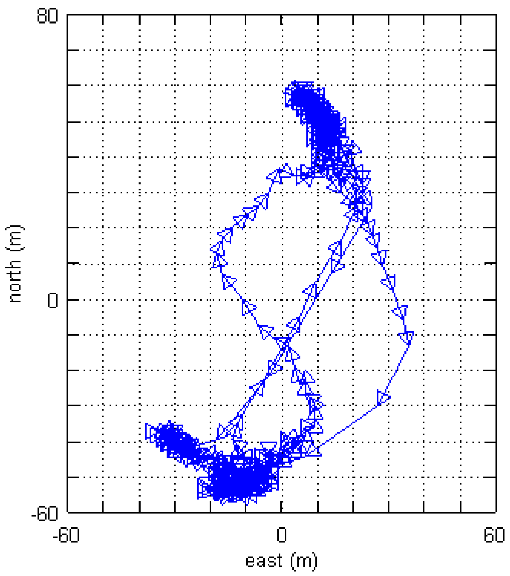


GPS buoy positions during a field test in 14 m deep water off the Dutch coast, near IJmuiden. Two clusters of points can be discerned, corresponding with flood tide (North) and ebb tide (South).

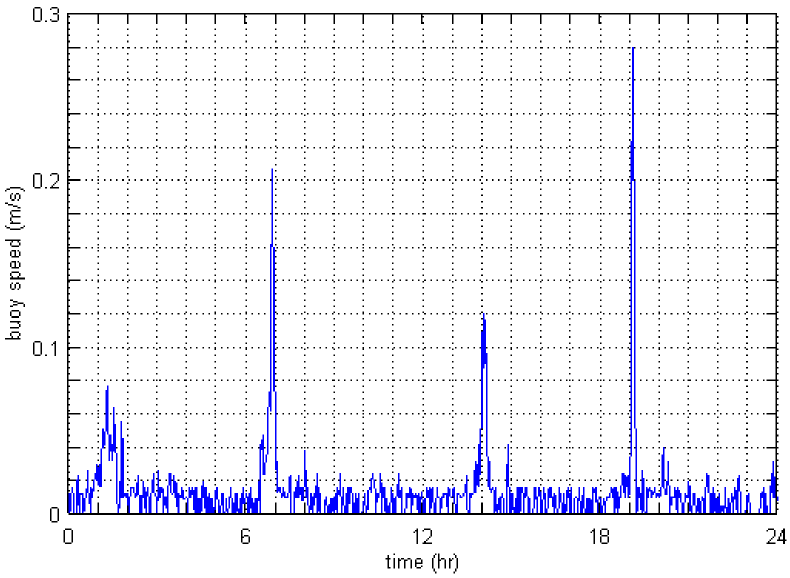


Buoy speed during field test

# DWR4 with ACM

Datawell - Oceanographic Instruments

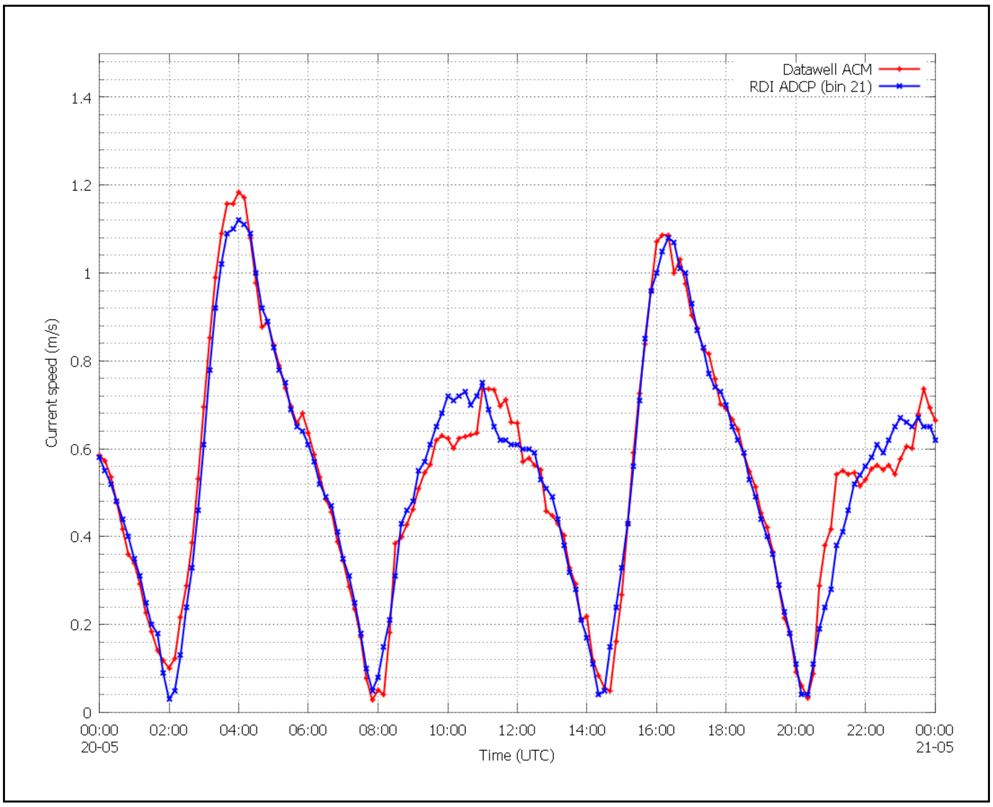


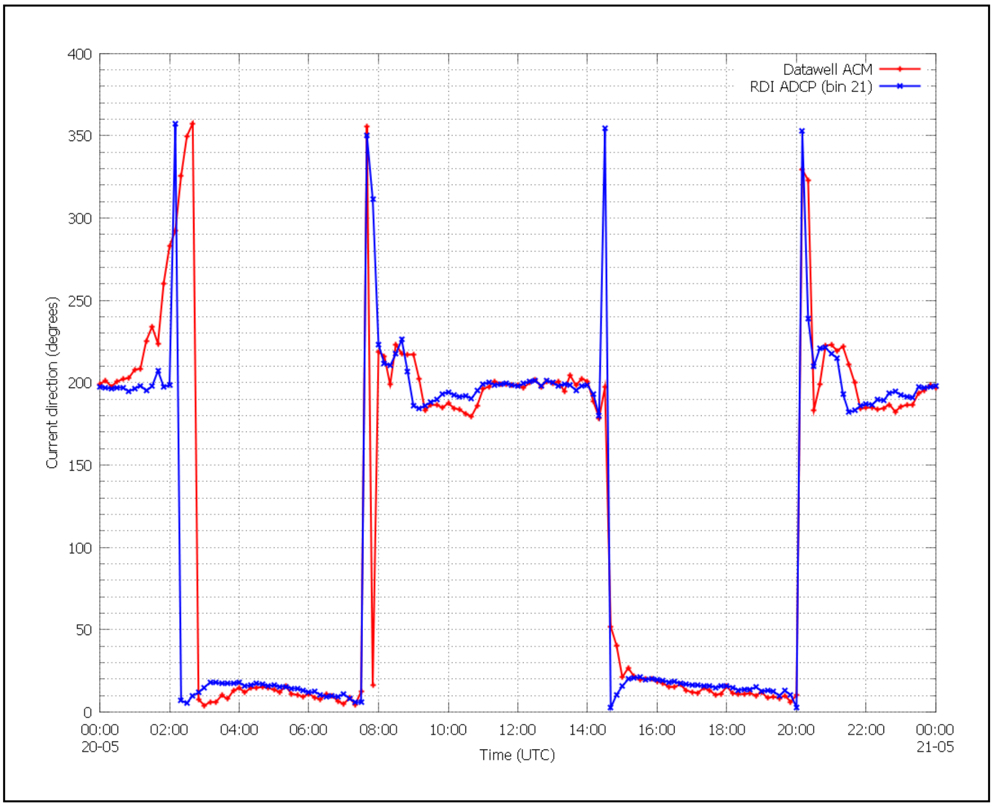

### Fouling

The main reason for low signal to noise ratio of the received acoustic signal is fouling. In order to monitor the performance of the ACM, the RSSI of each transducer is determined and transmitted ashore.

Fouling after fourteen weeks at sea.

To reduce fouling on the hull, the user can apply an antifouling coating. This does not affect the quality of the current measurement. Care should be taken that the used antifouling does not interfere with the active surface which is made of epoxy.

Transducer hardly visible, still measuring.

Alternatively we offer a Cunifer10 hull to prevent fouling.

### Transducer damage

The basis of the ACM are the well proven acoustic sensors made by Reson. Their intrinsic robustness is ruggedized by placing them in recess in a stainless steel housing. Should the surface of the transducer yet get damaged, this does not inevitably lead to failure of the current measurements. Even severe damage of the surface turns out to be acceptable.

Recessed transducer in the hull.

In the hostile environment of the sea, vessel interference cannot always be avoided. Collisions with ships or boats may leave a bump or a dent in the hull, which in turn may destroy the initial transducer alignment. A mechanical realignment of the transducers may be no easy job, or even impossible. In order to meet this situation, the azimuth and elevation directions of the transducers can be recalibrated. The new alignment matrix is stored in the ACM memory.

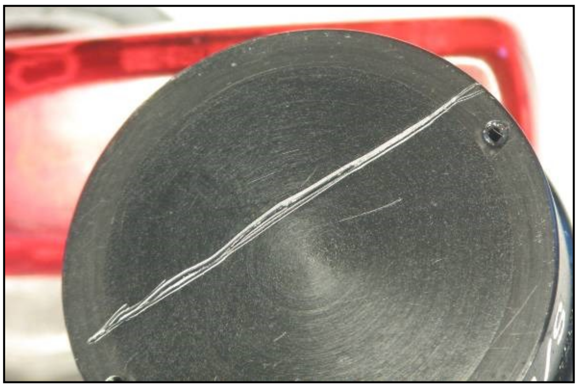

Severely damaged surface still measuring well. The scratch is 0.3 mm wide and 0.2 mm deep.




Datawell BV
Zomerluststraat 4
2012 LM Haarlem
The Netherlands

T +31 72 534 52 98
F +31 72 572 64 06
E sales@datawell.nl
W www.datawell.nl

# DWR4 with ACM

Datawell - Oceanographic Instruments

A perfectly floating buoy in water with a constant current profile, is not expected to measure vertical water velocity. A sudden change of measured vertical velocity may be indicative of a serious transducer misalignment, due to e.g. vessel interference, or of other incidents that necessitate service to the system.

**Preparing the DWR with ACM**

Prior to launching the DWR, some preparations are required. In case the hull needs to be sandblasted and/or painted, the acoustic transducers can be replaced by dummies to avoid damage. Three grey dummies are supplied with the buoy, as well as a special tool for removing and (re)mounting the transducers.

To protect the Hippy-40 sensor a triangle can be placed on the fender of the buoy.

**Power switch feature**

A power switch on the hatch cover of the DWR4/ACM is now a standard feature. Switching off the power starts the procedure of closing and storing the current data file on the data logger. Data stored on the data logger is retained when the buoy is switched off or when the batteries are removed.

The actual switch is covered by a small watertight dome that can be opened and closed with a standard 19 mm wrench, identical to the wrench for the standard Datawell 12 mm D-shackle in the mooring.


**Solar option**

For extension of the operational life of the DWR4/ACM, a solar panel plus boostcaps can be installed. Solar energy will power the DWR4/ACM, the surplus energy is stored in boostcaps. When solar energy is not sufficiently available, energy is used from the boostcaps. When they are depleted, the primary batteries are used.


**Satellite communication**

Iridium SBD or Argos satellite system can help to retrieve a buoy that has broken from its mooring and can relay the measured wave and current data.

**Operational issues**

An eye-catching difference between the DWR4/ACM and its predecessors is the mooring eye no longer being placed "at the south pole", on the axis of symmetry, but somewhat higher up, on the 'meridian' of one of the transducers. This symmetry breaking gives the spherical buoys for the first time a kind of 'bow' and 'stern'. The asymmetric mooring eye limits the buoy's average pitch, thus keeping the buoy upright and the acoustic transducers underwater even in high current conditions.

In operation the DWR4 with ACM option is very similar to the DWR MkIII:

- The layout of the mooring line is identical.
- A triangle is strongly recommended in order to avoid damage to the Hippy40 sensor.
- The HF range is identical.

# DWR4 with ACM

Datawell - Oceanographic Instruments

## Specifications

| | | |
|---|---|---|
| **Current Meter** | General | Method: Doppler<br>Cell size: 0.4 m - 1.1 m from surface<br>Update rate: every 10 minutes<br>Sensors: three 2 MHz acoustic transducers |
| | Speed | Range: 0 - 3 m/s, resolution: 1 mm/s<br>Accuracy: 1% of measured value +/- 2 cm/s<br>Std. (1σ): 1 - 3 cm/s (depending on wave height) |
| | Direction | Range: 0° - 360°, resolution 0.1°<br>Accuracy: 0.4° - 2° (depending on latitude) typical 0.5°<br>Reference: magnetic north |
| **Wave sensor** | Type and processing | Type: Datawell stabilized platform sensor<br>Sampling: 8-channel, 14bit @ 5.12 Hz<br>Data output rate: 2.56 Hz<br>Processing: 32bits microprocessor system |
| | Heave | Range: –20 m - +20 m, resolution: variable, 1 mm smallest step<br>Accuracy: < 0.5% of measured value after calibration<br>< 1.0% of measured value after 3 year<br>Period: 1.0 s - 30 s |
| | Direction | Range: 0° - 360°, resolution: 0.1°<br>Heading error: 0.4° - 2° (depending on latitude) typical 0.5°<br>Period: 1.0 s - 30 s (free floating)<br>1.0 s – 20 s (moored)<br>Reference: magnetic north |
| **Other** | Water temperature | Range: –10 °C - +50 °C, resolution: 0.01 °C<br>Sensor accuracy: 0.1 °C<br>Measurement accuracy: 0.2 °C |
| | Integrated data logger | Compact flash module 1024Mb - 2048Mb |
| | LED Flashlight | Antenna with integrated LED flasher, colour yellow (590 nm), pattern 5 flashes every 20 s. |
| | GPS position | 50 channel, update every 10 min, precision < 5 m |
| | Datawell HF link | Frequency range 25.5 - 35.5 MHz (35.5 - 45.0 MHz on request)<br>Transmission range 50 Km over sea, user replaceable.<br>For use with HVA compatible Datawell RX-C4 receiver. |
| **General** | Power consumption | 500mW |
| | Batteries | 0.7m diam. Operational life 10 months<br>0.9 m diam. operational life 1.6 years |
| | Material | Stainless steel AISI316 or Cunifer10 |
| | Weight | Approx. 109 Kg 0.7m AISI316, 113 Kg 0.7m Cunifer10 |
| | | Approx. 192 Kg 0.9m AISI316, 201 Kg 0.9m Cunifer10 |
| | Power switch | Data files are closed and secured |
| **Options** | Solar power system | Solar panel combined with Boostcaps capacitors<br>Peak power:5 W Capacity: 2WH |
| | Iridium SBD/Argos | Satellite communication |
| | Hull diameter | 0.7m (excluding fender) 0.9m (excluding fender) |
| | Hull painting | Brantho Korrux “3 in 1”paint system (no anti-fouling) |

Datawell BV
Zomerluststraat 4
2012 LM Haarlem
The Netherlands



T +31 72 534 52 98
F +31 72 572 64 06
E sales@datawell.nl
W www.datawell.nl

# RX-C receiver

Datawell - Oceanographic Instruments

## Advanced HF link receiver with synthesizer tuner, network connectivity and HVA support


The RX-C is a dedicated HF link receiver that supports all Datawell Waverider buoys fitted with the standard HF transmitter. The RX-C supports both the “HXV” format and the “HVA” transmission formats. The HXV format is used by all buoys, except the DWR4 buoy which uses the HVA format.

In the RX-C, a programmable digital frequency synthesizer makes it possible to manually select the reception frequency in 100 Hz steps. This allows reception of any frequency between 25.5 and 35.5 MHz by the touch of a button. Additionally, up to 6 frequencies can be stored into the internal preset memory.

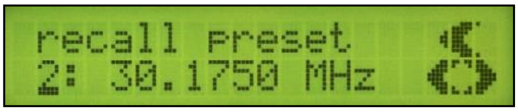


To connect the RX-C to a personal computer, the RX-C features both a serial port and an Ethernet network port. The serial port is ideal for a direct connection to a nearby PC. The Ethernet port allows the RX-C to be connected to a network or Internet router.

The Ethernet port makes the RX-C very flexible. The Ethernet port functions as four “virtual” serial ports. Once connected to a network or the internet, data can thus be retrieved from the RX-C by up to four computers at the same time. Also, a built-in embedded web server makes it possible to remotely monitor and configure the RX-C. This makes the RX-C ideal for application at remote locations.

To ensure the best reception possible, the RX-C uses a completely linear signal processing chain that does not distort the signal like traditional FSK receivers. This makes the RX-C relatively resistant against near-band interference and noise signals.

# RX-C receiver

Datawell - Oceanographic Instruments

The RX-C is supported by the W@ves21 software package and the new Waves4 package.

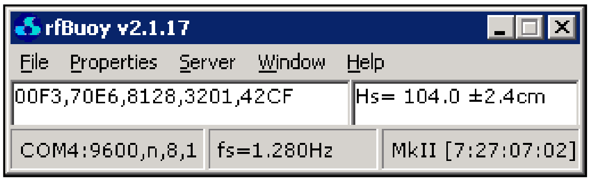


The RX-C comes standard as a compact desktop model. Alternatively, the RX-C is available as a 19" rack-mount model with the same specifications.
For applications where AC power is not available, such as remote (solar powered) locations, the RX-C can also be equipped with a 10 - 18 VDC power input instead of the standard 100 - 240 VAC power input.

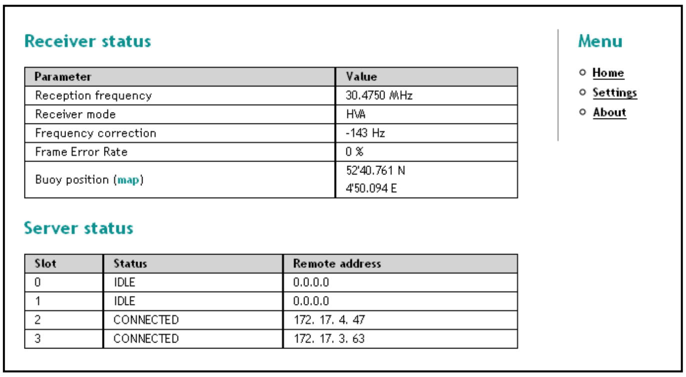


Embedded webserver

## Specifications

| | | |
|---|---|---|
| **HF** | Frequency range | 25.5 - 35.5 MHz ( 35.5 - 45.0 MHz on request )<br>PLL synthesizer tuning |
| | Usable sensitivity | –116 dBm (0.5 µV) |
| | Dynamic range | > 60dB |
| | Receiver bandwidth | 1.2 kHz |
| | Link bit rate | 81.92 bits per second, 2FSK modulation (HXV mode)<br>163.84 bits per second, 4FSK modulation (HVA mode) |
| | Compatibility | Directional Waverider MkI, MkII, MkIII, DWR-G, WR-SG and DWR4/ACM |
| **Interface** | Display | 2 x 20 character liquid crystal display with backlight |
| | Network | RJ45 10base-T Ethernet |
| | Serial output | 3-wire RS232, 9600 bits per second |
| | AC power (standard) | 100 - 240 VAC, 50-60 Hz, 3.4W avg. / 5.0W max. |
| | DC power (optional) | 10 - 18 VDC, 3.0W avg. / 4.5W max. |
| **Environmental** | Temperature range | – 10 - +50 °C |
| | Relative humidity | 10 - 80% (non condensing) |
| | Weight (desktop) | 1.8 kg |
| | Weight (19") | 2.3 kg |
| | Dimensions (desktop) | 230 x 100 x 200 mm (W x H x D) |
| | Dimensions (19") | 482 x 88 x 200 mm (W x H x D) 2U (rack size) |

# Libdatawell

Datawell - Oceanographic Instruments

## Libdatawell: a software library for the DWR MkIII and DWR4

**Do you want to use Waverider data in your (proprietary) software? Just include the libdatawell software library that takes all the decoding work off your hands, and lets you focus in the processing and presentation part of your software.**

### Datawell software library

The libdatawell software library consists of the following parts:

- A library named libwaves, for decoding the data transmitted by the DWR MkIII, DWR-G(4), WR-SG, and DWR4 buoys and received by an RX-C receiver; libwaves can be included in other, proprietary, software projects.
- A set of rudimentary tools based on this library that performs a basic conversion of the DWR MkIII, DWR-G(4), WR-SG, and DWR4 data into CSV files.
- Specifications of the data formats used.

### Introduction

Libwaves helps you develop your own software or analysis tools for all types of Datawell buoys. It aims at two groups of users:

- Users who want to develop their own processing or presentation software in e.g. C. This group of users can use the library directly. For these users the development headers are available, allowing use of the library in any computer language that can call functions in a library written in C.
- Users who want to analyse the wave data in programs like Matlab, Octave or Excel. For these users the library contains the tools to receive, log and convert the data of the buoy to CSV files. These files can be opened and read by the aforementioned programs to process and plot the data in spreadsheets and charts.

### Formats

The library contains decoding support for most common data types used by the Datawell buoys:

- HXV, the data transmitted via the HF-link by the DWR MkIII, DWR-G(4), and WR-SG buoys.
- RDT, the real-time data stored on the logger card of the DWR MkIII, DWR-G(4), and WR-SG buoys.
- SDT, the spectral and system data stored on the logger card of the DWR MkIII, DWR-G(4), and WR-SG buoys.
- HVA, the data transmitted via the HF-link by the 4-series of buoys.
- BVA, the stored on the logger card by the 4-series of buoys.
- SBD the e-mail format transmitted with Iridium *S*hort *B*urst *D*ata by the 4-series of buoys.
- Argos e-mail messages transmitted by the 4-series of buoys.
- The data received via iBuoy. Data received via the Internet using Iridium or GPRS.

The library contains the tools to convert these data formats to CSV files, allowing further processing with standard software.

For developers the library contains the engines to do these conversions and make the data available in C structures, allowing further processing with their own software.

| | A | B | C | D |
|---|---|---|---|---|
| 1 | Timestamp [-] | Datastamp [-] | latitude [rad] | longitude [rad] |
| 2 | 1307371212 | 31788 | 0.913998688 | 0.080638484 |

A CSV file with a GPS-location decoded from a BVA file

Datawell BV
Zomerluststraat 4
2012 LM Haarlem
The Netherlands



T +31 23 531 60 53
F +31 23 531 19 86
E sales@datawell.nl
W www.datawell.nl

# Libdatawell

Datawell - Oceanographic Instruments

**Contents of the package**

The library is shipped including the following components:

- The library itself.
- C/C++ development headers, used to develop software using the library.
- A set of tools including:
  - Saving the HXV data in CSV files.
  - Saving the RDT data in CSV files.
  - Saving the SDT data in CSV files.
  - Receiving the HVA data from a RX-C receiver over the network.
  - Logging the received HVA data.
  - Converting the BVA data on the logger into HVA data.
  - Saving the HVA data in CSV files.
  - Saving SBD e-mail messages in CSV files.
  - Saving Argos e-mail messages in CSV files.
- A set of documentation:
  - The manual describing the library and its tools.
  - The DWTP specifications.
  - The CSV specifications.
  - The iBuoy protocol specifications.
- Several BVA and HVA sample files.

**Availability**

The library is available for both the Windows and Linux platform. It is available free of charge. The library is shipped under a liberal licence, allowing you to redistribute the library and its tools with your own software. In order to receive a copy of the library, please contact our sales department.

| | A | B | C | D |
|---|---|---|---|---|
| 1 | status [-] | heave [m] | north[m] | west[m] |
| 2 | g | -0.066229668 | -0.006000172 | -0.103874241 |
| 3 | g | -0.019005474 | 0.038043804 | -0.118282322 |
| 4 | g | -0.059164034 | 0.085490935 | -0.136972025 |
| 5 | g | -0.135928402 | 0.118282322 | -0.14954809 |
| 6 | g | -0.114154993 | 0.084473792 | -0.123454264 |
| 7 | g | -0.041055023 | 0.017003921 | -0.067240274 |
| 8 | g | -0.017003921 | -0.022008498 | -0.022008498 |
| 9 | g | 0.040051093 | -0.034031374 | -0.020006385 |
| 10 | g | 0.155874248 | -0.011001062 | -0.066229668 |
| 11 | g | 0.173947912 | 0.055132868 | -0.120349365 |
| 12 | g | 0.083457053 | 0.092622673 | -0.133843103 |
| 13 | g | 0.047082897 | 0.041055023 | -0.102848982 |
| 14 | g | 0.047082897 | -0.047082897 | -0.064209403 |
| 15 | g | -0.043063477 | -0.111065252 | -0.031023779 |
| 16 | g | -0.144296031 | -0.151653892 | 0.019005474 |
| 17 | g | -0.100799937 | -0.175018319 | 0.08142477 |

CSV file with the displacements decoded from a HVA file

## System requirements

| | | |
|---|---|---|
| **Minimum** | OS | Debian Linux<br>• Wheezy i386 / amd64<br>• Jessie i386 / amd64<br>Ubuntu Linux*<br>• Precise Pangolin i386 / amd64<br>• Trusty Tahr i386 / amd64<br>Window<br>• Windows Vista<br>• Windows 7 |
| | CPU | 80x86 compatible with the SSE2 instruction set |

*) For other Linux distributions contact our sales department.

Waves4

Datawell - Oceanographic Instruments

## Monitoring Software Waves4

**The software for the analysis, processing, and displaying of wave data from the Datawell Waverider buoys.**

### Introduction

The Waves4 suite contains a set of programs for data acquisition, processing and presentation of the Datawell Waverider buoys.
It provides detailed 2D plots of wave data for analysis and research. It also provides overviews of the latest measurements in a list overview. Real-time data is displayed. Parameters are stored and made available for post-processing.

### Data acquisition

The Waves4 suite contains a data acquisition background process (Windows: service, Linux: daemon) named buoyd. This background process receives the data over the HF-link from a RX-C receiver. It is also able to receive the e-mail messages – for the 4-series of buoys – received from the Iridium Short Burst Data system. For the 4-series of buoys it is also possible to receive data via Argos or iBuoy (an Internet connection via Iridium or GPRS).

### Data processing

The buoyd background process sends the received data to the processing background process, named waved. It stores, decodes and processes the received data from multiple buoyd instances. The decoded data is stored in an internal cache.

### Data presentation

Presentation of the wave data is taken care of by the Waves4 program itself. This program receives the data from the waved module and displays it. Due to the cache in waved it is possible to immediately view historical data along with current data. The data is presented in a tabular interface, where every tab sheet contains one or more widgets.

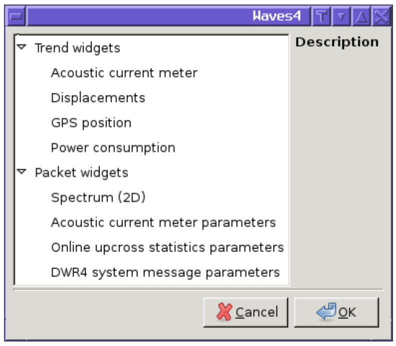


Every widget displays a set of data of the buoy, either as a parameter list or as a trend plot. Trend plots show a set of related data and allow the user to select signals of interest. For example, the spectral statistics widget, by default, shows the Hs along with the Tz.
Checking the corresponding checkbox in the settings

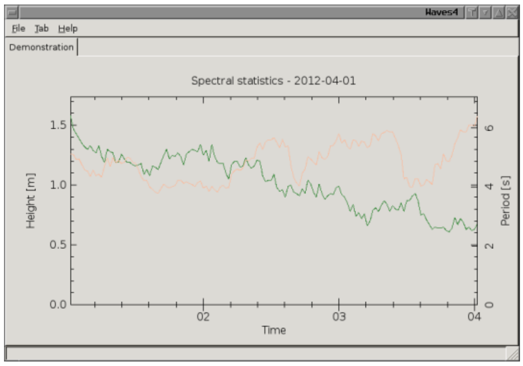


dialogue adds the $T_p$ signal. Unchecking the $H_s$ box allows showing the wave direction instead. Multiple widgets can be added to a tab sheet and configured individually.

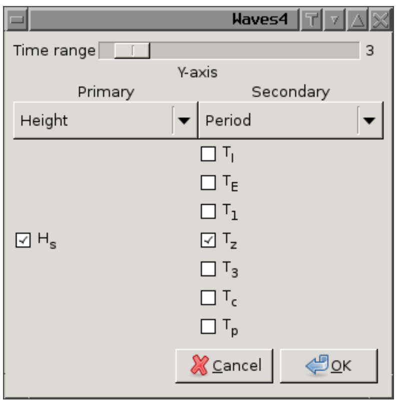




Datawell BV
Zomerluststraat 4
2012 LM Haarlem
The Netherlands

T +31 72 534 52 98
F +31 72 572 64 06
E sales@datawell.nl
W www.datawell.nl

# Waves4

Datawell - Oceanographic Instruments

### Sea-state monitoring

The Waves4 program can be extended with the monitoring module, intended to serve users involved in operational situations (port authorities, offshore companies). This module allows instant assessment of the sea state. Its settings dialogue allows choosing from a variety of sea-state parameters, for example: $H_s$, $T_z$, $H_{max}$, and many more.


Every parameter is attributed zero or more thresholds. These thresholds determine the colour of the parameter pane, this allows for a fast evaluation of the sea-state and whether or not the current situation requires attention.

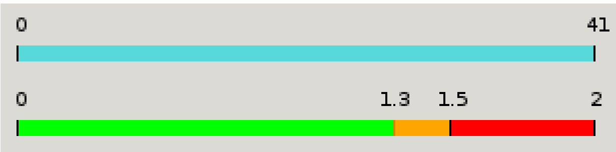


### Configuration

For configuring the Iridium Short Burst Data (SBD), Argos, and iBuoy settings the Waves4 suite has a configurator program, named Waves4-configurator. Modifications made here are sent to the DWR4 buoy, allowing you to easily control the buoy's mode of operation.

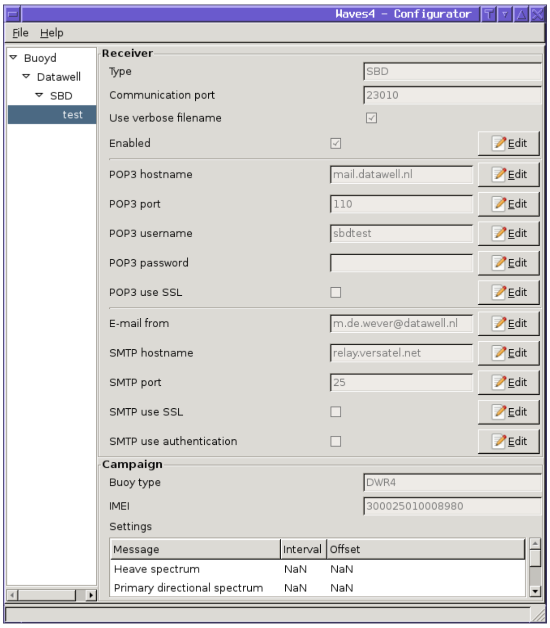


## System requirements

| | | |
|---|---|---|
| **Minimum** | OS | Debian Linux<br>• Wheezy i386 / amd64<br>• Jessie i386 / amd64<br>Ubuntu Linux*<br>• Precise Pangolin i386 / amd64<br>• Trusty Tahr i386 / amd64<br>Window<br>• Windows Vista<br>• Windows 7 |
| | CPU | 80x86 compatible with the SSE2 instruction set |
| | Display | At least 1024x768 larger recommended |

*) For other Linux distributions contact our sales department



Datawell BV
Zomerluststraat 4
2012 LM Haarlem
The Netherlands

T +31 72 534 52 98
F +31 72 572 64 06
E sales@datawell.nl
W www.datawell.nl

# Acoustic Current Meter

Datawell - Oceanographic Instruments

## Sea trial acoustic current meter


### Abstract

This report describes the results of the three-month sea trial of the DWR4/ACM, the new Directional Waverider with Acoustic Current Meter. The quintessence of the DWR4/ACM is its capability of measuring surface current with the ease of a buoy, and corrected for the buoy motion. The trial off the coast of IJmuiden, near a measurement site of RWS that was used as a reference station, was the final test in the research and development stage of the instrument. The results are in excellent agreement with the reference, and the DWR4/ACM performed well as to both robustness and reliability.


### Introduction

The Datawell acoustic current meter (ACM) has been at sea for 103 days. The sea trial lasted from 18 May 2011 until 26 August 2011. On 26 August the buoy was hit by a ship and drifted to shore.

Because of the size of the dataset, two days are chosen to be presented in detail. The first day is 20 May 2011 and the second day is 14 July 2011. These two days are chosen because they span a range of significant wave height (Hs): on 20 May 2011 this was approximately 50 cm and on 14 July 2011 it was approximately 450 cm. Aggregate results for the sea trial will be shown after these two days are discussed. Graphs of the measured current speed and direction of all 103 days are shown in the appendix.

### Location

The buoy was anchored approximately 1 km west of IJmuiden, The Netherlands. A map with the measurement location and the surrounding area is shown in Figure 1. This area has heavy shipping traffic but also located here is a measurement site of Rijkswaterstaat. This site has two upward facing RDI Workhorse Monitor 1200 kHz ADCPs, which makes it an ideal reference for our measurements. Also available from this site are parameters such as wind speed and water level. The buoy was located 100 m from the measurement site of Rijkswaterstaat.


Datawell BV
Zomerluststraat 4
2012 LM Haarlem
The Netherlands

T +31 23 531 60 53
F +31 23 531 19 86
E sales@datawell.nl
W www.datawell.nl


**Figure 1** Map showing the approximate location of the buoy and the measurement site (both at the green arrow). Notice the breakwaters extending into the North Sea.

### Weather

During the sea trial, the weather has varied substantially. Especially important for the analysis of ACM data are the knowledge of wind speed and the significant wave height. This is because the ACM measures currents 1 m below the surface where the influence from the aforementioned two variables is present.

Winds were predominantly from the westerly direction, varying from south to north. Average wind speed during the sea trial was 7.5 m/s, with frequent spikes up to 15-20 m/s. This has resulted in calm periods, with $H_s$ = 50 cm, and stormy periods with $H_s$ = 450 cm. Detailed wind speeds and significant wave height for the sea trial are shown in Figure 2 and Figure 3.

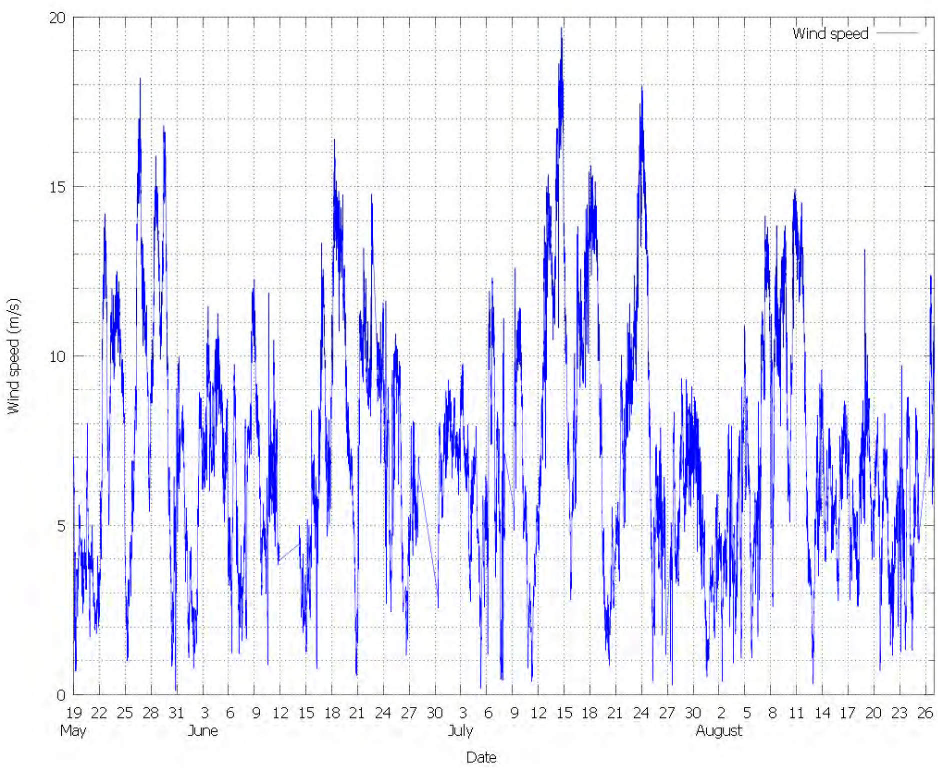


**Figure 2** Wind speeds at the measurement site of Rijkswaterstaat during the sea trial. Some data is missing, which is shown as straight lines.

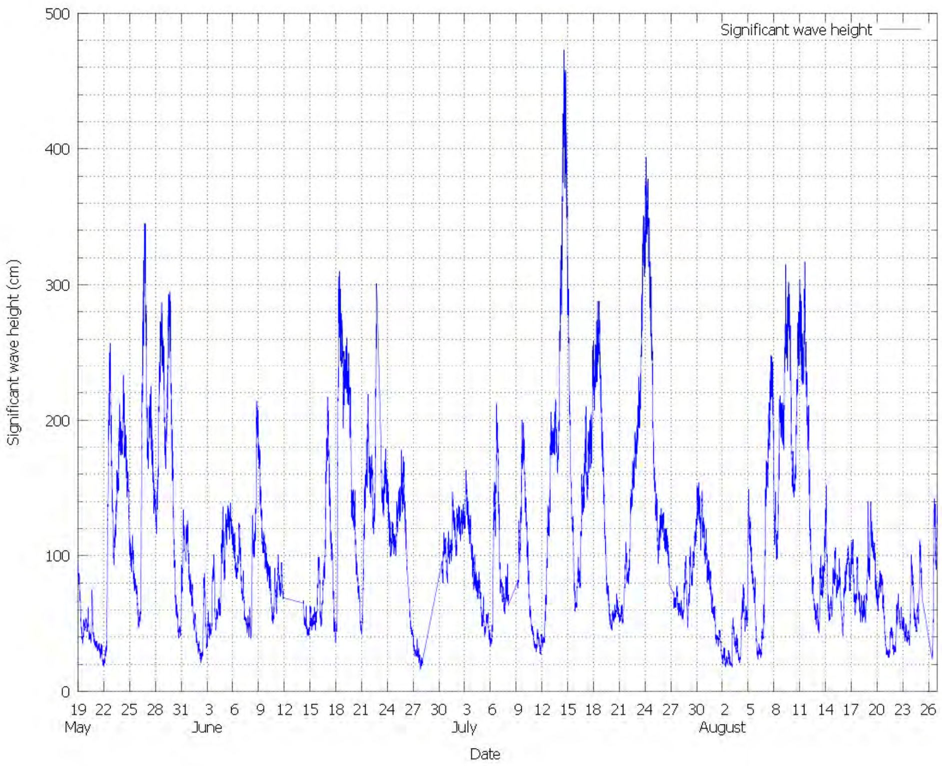


Figure 3 Significant wave height at the measurement site of Rijkswaterstaat during the sea trial. Some data is missing, which is shown as straight lines.

Two other important parameters for the ACM are the water temperature and the salinity. These are used to calculate the speed of sound in the sea, which is used for the calculation of the current speed and direction. The water temperature is measured by the buoy itself and salinity has been set at 35 per mil. The water temperature steadily rose during the sea trial from 14 °C to 19 °C.

## Comparison between Datawell ACM and RDI Workhorse monitor

A direct comparison between the two instruments is not without pitfalls. First, there is the distance between the location of the buoy and that of the measurement site of Rijkswaterstaat. Second, the ADCP measures at one location, whereas the buoy "goes with the (tidal) flow", northward and southward. Third, there are structures nearby that may induce strong local fluctuations in flow patterns. And, last but not least, the Datawell ACM measures currents approximately 0.5-1 m below the surface, whereas the RDI Workhorse Monitor measures currents anywhere but that depth.

In the configuration of Rijkswaterstaat, the RDI Workhorse Monitor measures current speed and direction in 28 bins of 0.5 m size. The covered depth is from -13.75 m N.A.P.[1] through -0.25 m N.A.P. Because of the tides, the upper bins are at times above sea level.

[1] N.A.P. is the reference level in use in The Netherlands.

The sea level varies with the tide between -0.60 m N.A.P. and +0.80 m N.A.P. Theoretically, the reference bin for the Datawell ACM would be 1 m below the sea surface. However, the sea level is also influenced by waves. With large significant wave height, the instantaneous sea level could be lower. Therefore, the chosen reference bin should be somewhat deeper than 1 m below the sea surface.

In this report, bin 21 is chosen as reference bin. This bin is at -3.75 m N.A.P, which is generally 3 m to 4 m below the sea surface. This bin is always under water and therefore has consistent results for comparison.

The following agreements as well as differences between the results of the two instruments must thus be weighed with these caveats in mind.

Differences between the instruments in frequency of maintenance, collision risk, or susceptibility to fouling or siltation are not reflected directly in the results.

20 May 2011

The comparison of current speed and current direction on 20 May 2011 are shown in Figure 4 and Figure 5.

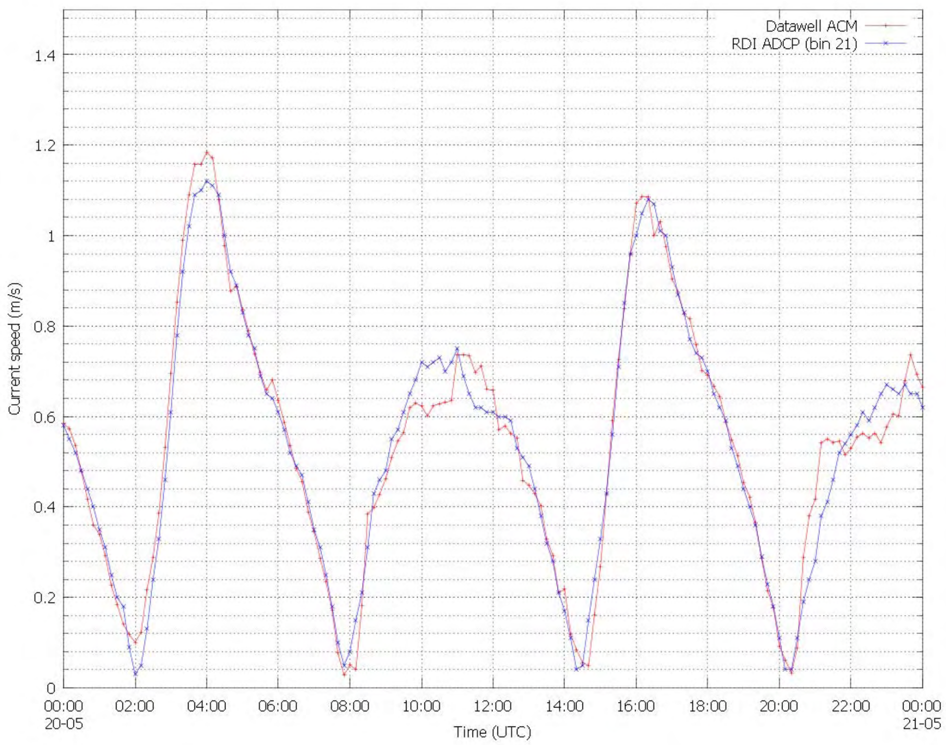


**Figure 4** Measured current speed from Datawell ACM and RDI Workhorse Monitor (bin 21, depth -3.75 m N.A.P.) on 20 May 2011.

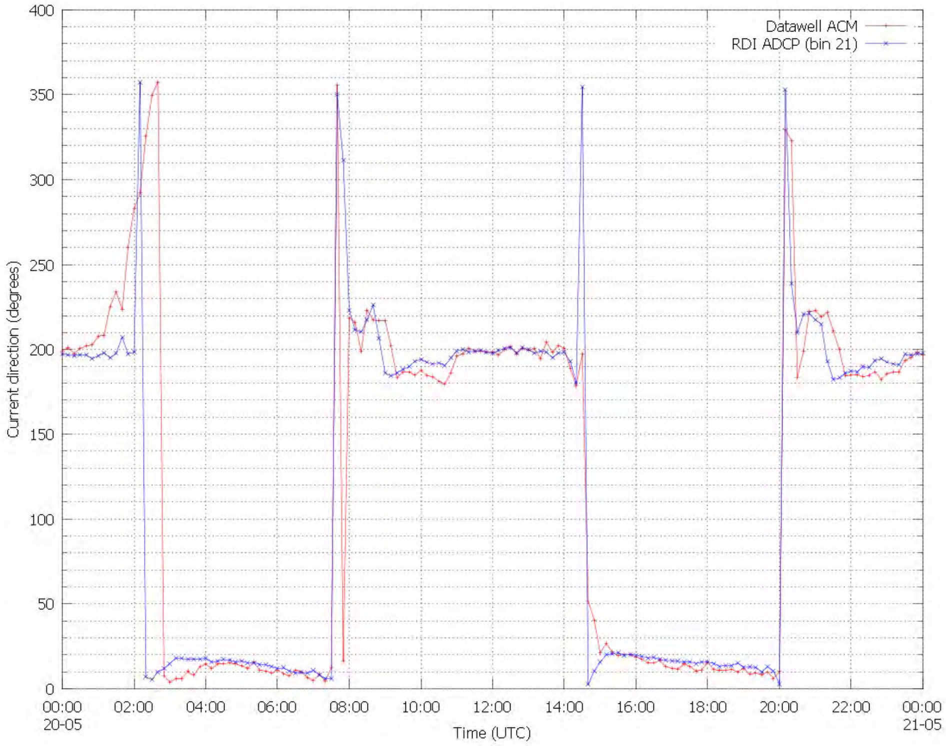


**Figure 5** Measured current direction from Datawell ACM and RDI Workhorse Monitor (bin 21, depth -3.75 m N.A.P.) on 20 May 2011.

Figure 4 shows multiple minimum and maximum values in the current speed during the day. These are caused by the tide. The strongest currents, at 04:00 and 16:00, are during high tide and the smaller peak values are during low tide. The smallest currents occur during the change in tides (slack tide).

For the most part, the current measured by the Datawell ACM is equal to the current measured by the RDI ADCP. However, some differences between the Datawell ACM and the RDI ADCP are visible.

One such difference between the Datawell ACM and the RDI ADCP can be seen at 04:00. This difference is due to the difference in measurement depth between the Datawell ACM and the RDI ADCP. This can be seen when the other bins are plotted in the same figure. This is shown in Figure 6. In the figure, it can be seen that the current speed increases when the bins approach the surface. Shown are bins 21 through 24, where bin 24 is closest to the surface and has the current speed which has the best match with the Datawell ACM. Bin 25 and higher are not shown, because they have inconsistent current speed due to their presence close to the surface. Notice the difference in current speed that can exist between bins.

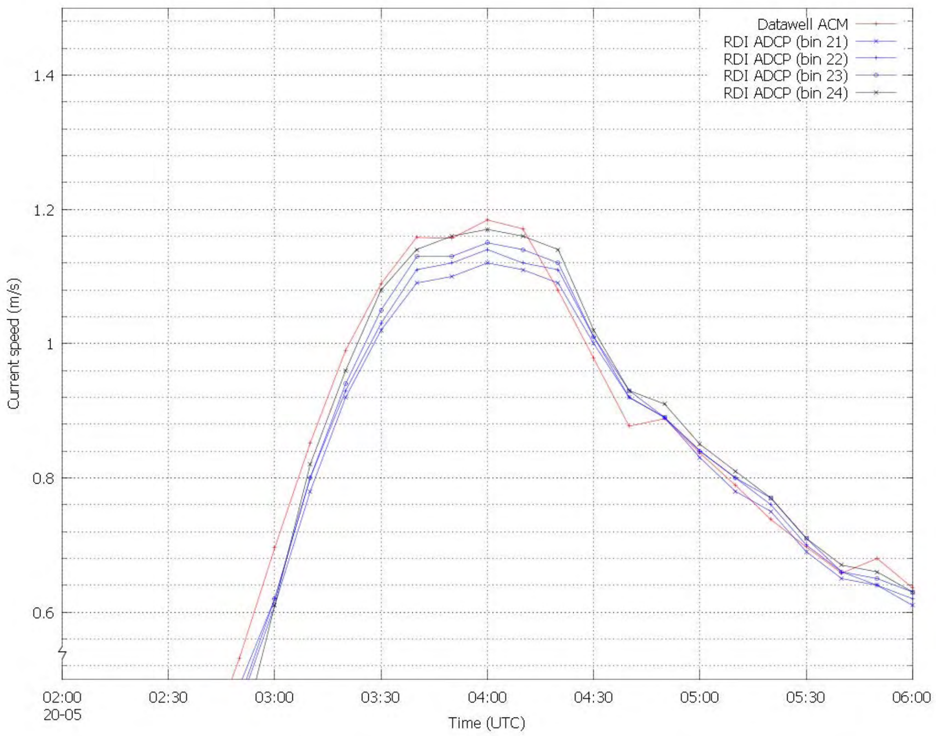


**Figure 6** Detailed view of the current speed on 20 May 2011 between 02:00 and 06:00. Bin 21 is at a depth of -3.75 m N.A.P. and bin 24 is at a depth of -2.25 m N.A.P. The spacing between the bins is 0.5 m.

Another difference can be seen between 10:00 and 12:00. The Datawell ACM first measures less current speed than the RDI ADCP, after which the RDI ADCP measures a larger current speed than the Datawell ACM. Also, the direction of the current measured by the Datawell ACM has a slight shift to the west at the same time (Figure 5).

This difference is shown in detail in Figure 7. From 08:00 to 11:00, the difference can again be explained by measurement depth. It can be seen in the figure that the measurements from the bin closest to the surface, also is the bin which is closest to the measured current from the Datawell ACM. This leads to the assumption that if the RDI ADCP were able to measure close to the surface, the measured current speeds would be the same for all practical purposes.

The difference from 11:00 to 14:00 is more complicated to explain and probably has to do with the current profile at the measurement site. It occurs during multiple days in the sea trial. The difference is not due to depth, because the bins closest to the surface actually measure less than the bins closest to the bottom. As said before, the measurement site is located at a harbour entrance. This harbour entrance is protected by two breakwaters with a length of 1.5 km. The site is located 1 km from the tip of the breakwaters. Influence from these breakwaters can be present and generate a complex current profile with variation in currents at different locations. This also could explain the small difference between 20:00 and 0:00.

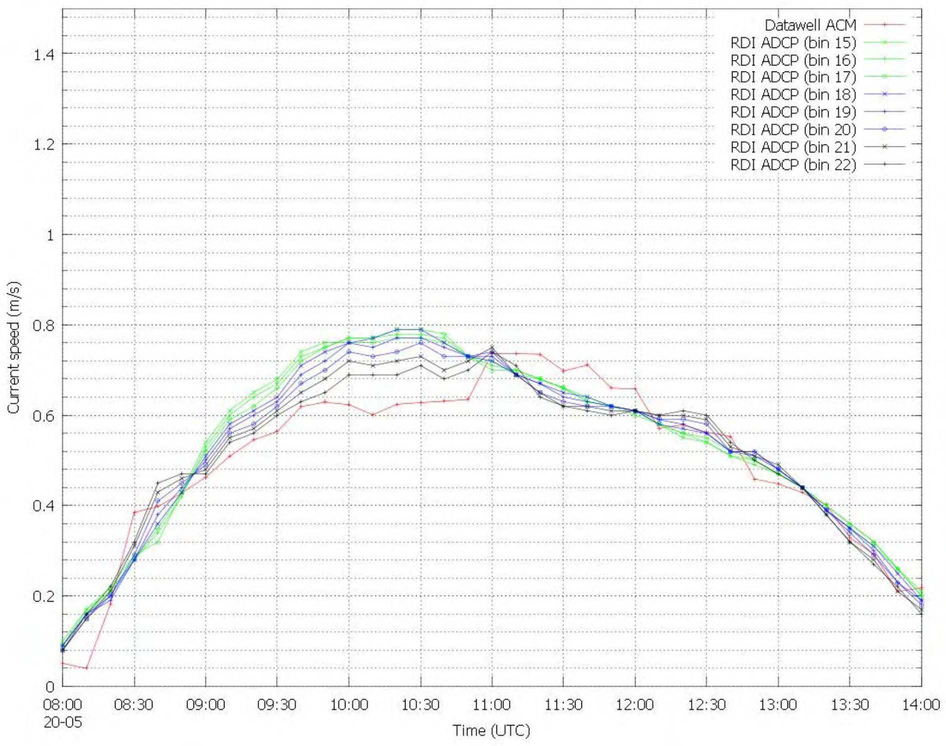


Figure 7 Detailed view of the current speed on 20 May 2011 between 08:00 and 14:00. Bin 15 is at a depth of -6.75 m N.A.P. and bin 22 is at a depth of -3.25 m N.A.P. The spacing between the bins is 0.5 m.

Another interesting time Figure 4 is the transition between high and low tide. The current reduces to zero and then picks up again. At these times the buoy crosses over from its ebb position to its flood position. During these crossings, the measurements may benefit from correction by GPS. However, in this experiment this was not yet implemented, hence the slightly different speeds at 2:00, 8:00, 14:00 and 20:00.

Figure 5 shows the direction of the current, as measured by the Datawell ACM and the RDI ADCP. In general, the current direction measured by the Datawell ACM follows the current direction measured by the RDI ADCP. At times, a delay can be seen between the two. This is due the difference in depth.

An analysis of the data from the RDI ADCP has shown that current direction can have tens of degrees difference between the surface and the bottom. Also it must be kept in mind that the direction has a cyclical nature, e.g. jumps between 0° and 359° are really only 1°. Furthermore, the surface layer is influenced by wind, which can create small differences from time to time.

14 July 2011

Figure 8 and Figure 9 show the comparison between the Datawell ACM and the RCI ADCP for 14 July 2011. This day had wind speeds in excess of 15 m/s coming from the northwest (300°). The resulting significant wave height was 400-450 cm.

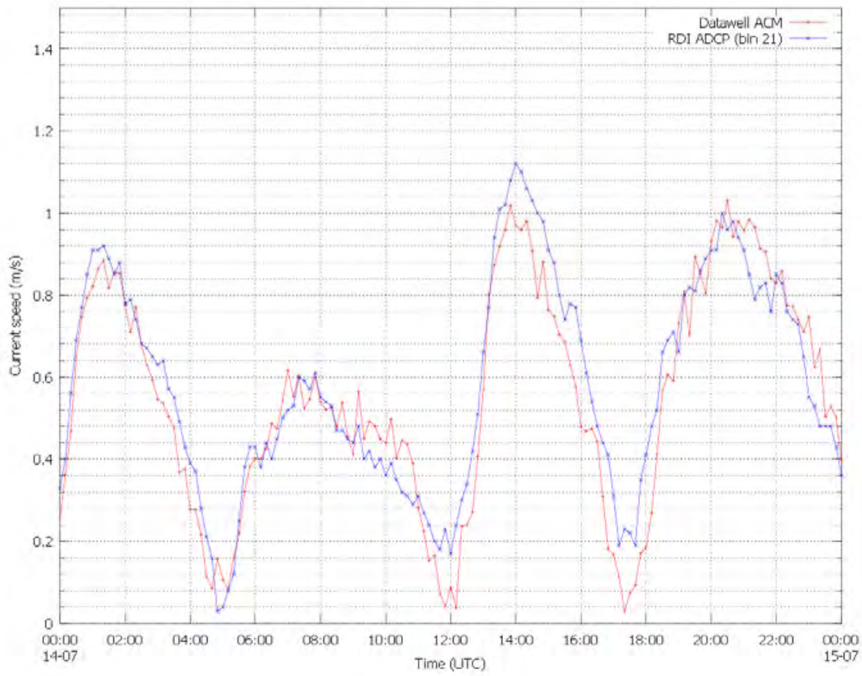


**Figure 8** Measured current speed from Datawell ACM and RDI Workhorse Monitor (bin 21, depth -3.75 m N.A.P.) on 14 July 2011.

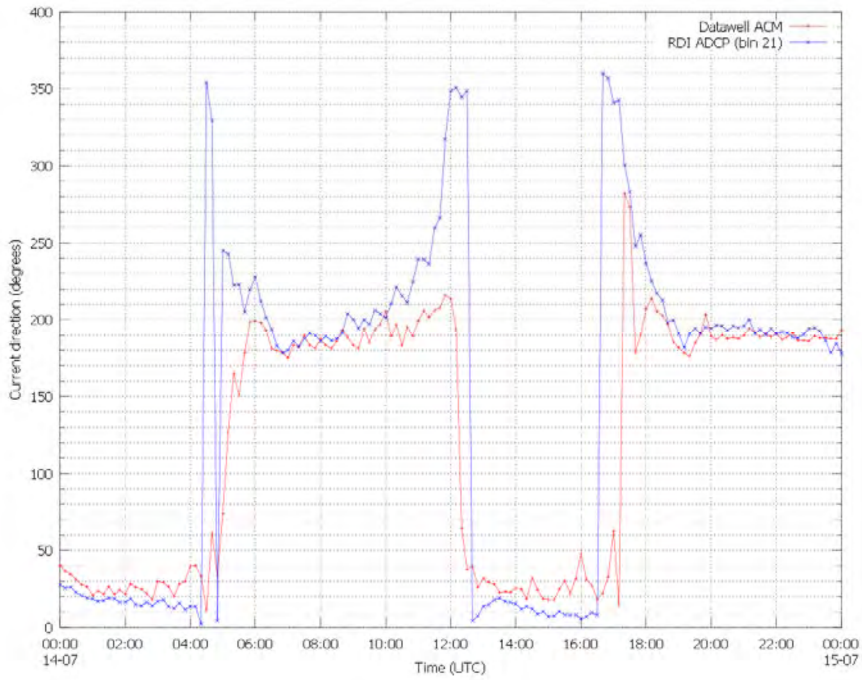


**Figure 9** Measured current direction from Datawell ACM and RDI Workhorse Monitor (bin 21, depth -3.75 m N.A.P.) on 14 July 2011.

These wave conditions clearly affect the current, as can be seen when Figure 8 is compared with Figure 4. The current speed and direction are less fluent but the measurements from the Datawell ACM and the RDI ADCP are, given the circumstances, still very similar.

The last two transitions, 12:00 and 17:00, stand out. The measured current speed by the Datawell ACM drops to zero whereas the current speed measured by the RDI ADCP remains at ≈0.2 m/s. The difference in measured current at 12:00 is caused by the difference in measurement depth. The difference at 17:00 is not directly related to the measurement depth. A substantial part of this difference is expected to stem from the drifting of the buoy itself. In the future, these gaps will be repaired by using the buoy GPS.

Furthermore, there is a difference between the Datawell ACM and the RDI ADCP from 14:00 to 17:00. More or less the same difference can be seen between 02:00 and 04:00. Figure 9 also shows the current direction to be somewhat more easterly at these times. This suggests influence from wind, as the wind originates from 300°. This is perpendicular to the current direction and apparently slows the current somewhat and changes its direction a little in comparison to the current far beneath the surface.

## Aggregate results

The aggregate results comprise 61 days of the 103 days, corresponding to 7977 measurements in total. During the other 42 days, the measurement site of Rijkswaterstaat was out of use because of maintenance.

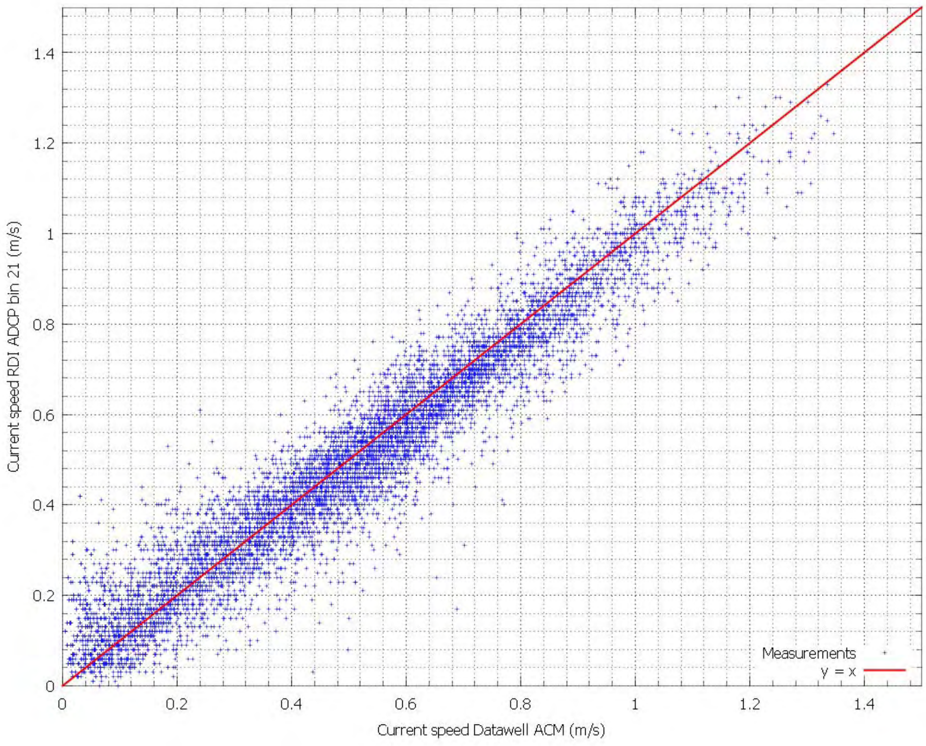


**Figure 10** Scatter plot of the Datawell ACM and RDI ADCP (bin 21, depth -3.75 m N.A.P.).

Figure 10 shows a scatter plot with the current speed as measured by the Datawell ACM against the current speed as measured by the RDI ADCP (bin 21). Also visible in the figure is a line showing a one-to-one relation between the two variables. The measurement cloud deviates a little bit from this one-to-one relation. As the depths between the two current measurement devices differ, some discrepancies can be expected. This is also evident from above presented comparisons. Also, the wind has a direct effect on the surface current. Unlike the deeper ADCP, the Datawell ACM measures both the tidal current and the wind-induced current. This has been visualized in Figure 11. Shown is a scatter plot of the differences in current speed during low tide between the Datawell ACM and the RDI ADCP against the direction of the wind.

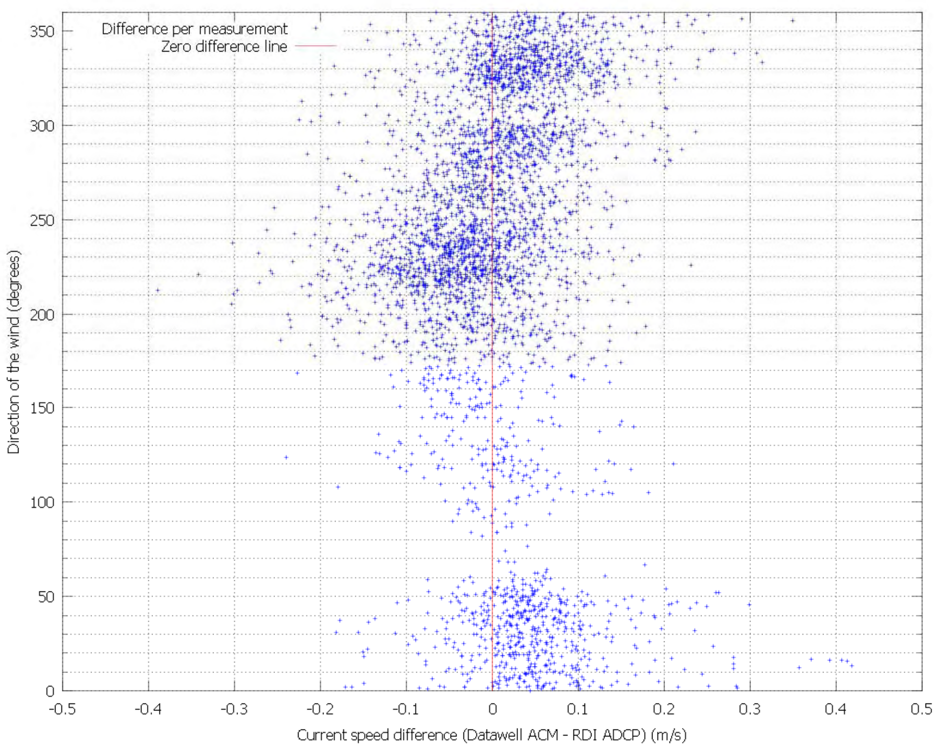


**Figure 11** Scatter plot showing the difference in current speed during low tide between the Datawell ACM and the RDI ADCP (bin 21, depth -3.75 m N.A.P.) shown against the direction of the wind.

During low tide, the buoy is located south of its anchor weight with a current flowing from north to south. A wind from the southwest (≈225°) will therefore reduce the current close to the surface and hence result in a lower current speed measurement for the ACM. Contrarily, winds blowing from the north will result in larger current speed measurement for the ACM. The wind effect is further established by regarding the results for high tide, as shown in Figure 12. The observed trend is of course the opposite of that in Figure 11, as now the current flows in the reverse direction.

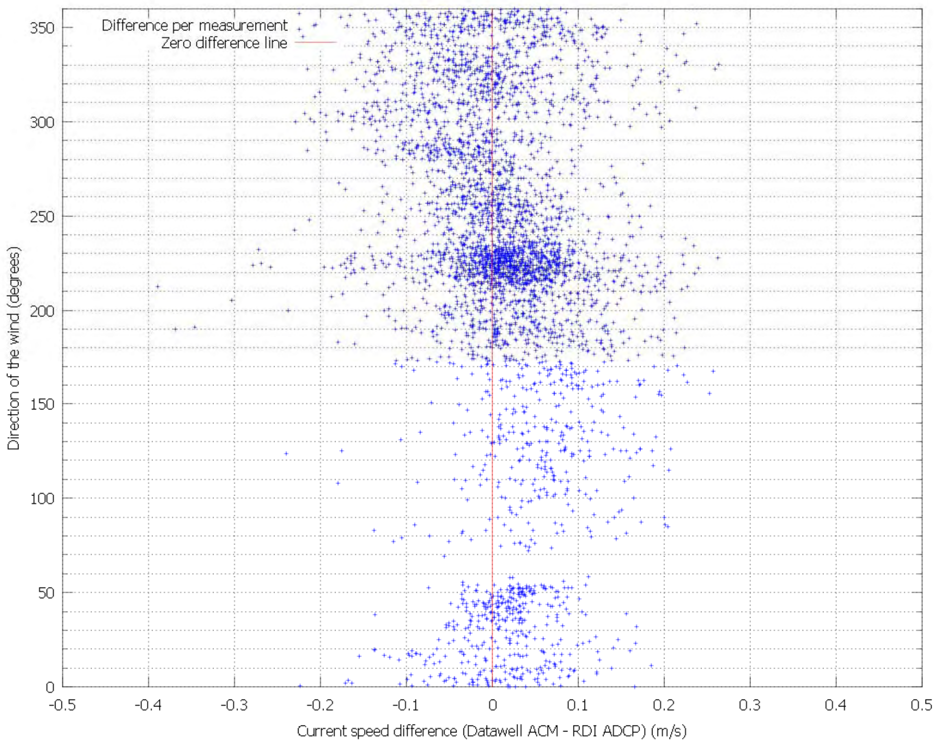


Figure 12 Scatter plot showing the difference in current speed during high tide between the Datawell ACM and the RDI ADCP (bin 21, depth -3.75 m N.A.P.) shown against the direction of the wind. Notice the reverse of the effect as shown in Figure 11.

## Fouling

This sea trial has also been an excellent opportunity to monitor the effect of fouling on the ACM. Figure 13 shows the buoy at the start of the sea trial. The transducers and the buoy were not treated with anti-fouling.

The buoy was inspected twice during the sea trial. The first inspection was after five weeks at sea. The buoy was lifted from its anchor and inspected on board a ship. A photo of the buoy after five weeks at sea is shown in Figure 14. The bottom halve and part of the top halve of the buoy were covered with a biofilm. This film could be easily wiped off, but care was taken to prevent this. Also visible in Figure 14 is the waterline as green/brown band on the upper halve.

The second inspection was done after fourteen weeks at sea (Figure 15). The buoy was again lifted from its anchor and inspected on board a ship. This time, the buoy was covered with long strands of brown and green fouling. These were present both on the top and bottom halve. The bottom halve was mainly covered with small shells, such as mussels and barnacles. An unmistakable difference was observed between the relatively unaffected forward-facing transducer, and the two backward-facing transducers that were hardly visible at the end of the trial. Apparently, the “up-current” side is less prone to fouling than the leeward side.

**Figure 13** The buoy equipped with the ACM before deployment. The transducers can be seen as dark circles at the left and right of the bottom halve of the buoy.

**Figure 14** The buoy after five weeks at sea. The fouling is limited to a biofilm.

**Figure 15** The buoy after fourteen weeks at sea. Green fouling is mainly present on the top half; brown fouling and small shells are present on the bottom half.

**Figure 16** A view of the front facing transducer after fourteen weeks. The transducer is visible as a black area within the red circle.

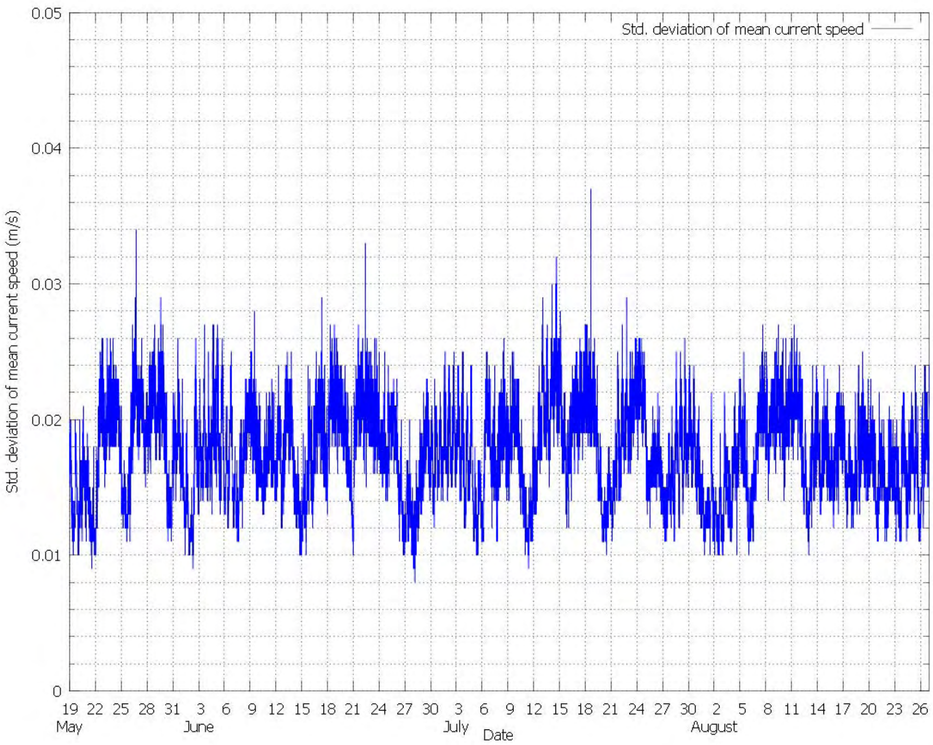


**Figure 17** Standard deviation of the mean current speed. The standard deviation of the mean current speed is calculated over 150 measurements.

## Measurement accuracy

The differences between the Datawell ACM and the RDI ADCP are small and can mostly be understood by the different measurement depths and locations. Shown in Figure 17 is the standard deviation of the mean current speed. This mean current speed is calculated over 150 measurements.

The standard deviation varies in time with the sea state. If the significant wave height is very small, e.g. 50 cm, the standard deviation approaches 1 cm/s. However, if the significant wave height increases to 450 cm, the standard deviation of the mean current speed increases to 2.6 cm/s. There are a few samples where the standard deviation is larger than 2.6 cm/s, but these are incidents.

In general, the standard deviation is well contained between 1 cm/s and 3 cm/s. This is worth mentioning considering the fouling near the end of the sea trial.

## Conclusion

The Datawell ACM has proven to be a reliable current measurement option for the sea surface layer. Fouling did not affect the quality of the measurement. Differences between the Datawell ACM and RDI ADCP can be attributed to four things: difference in measurement depth, measurement location, drifting of the buoy and measurement accuracies of both devices.

## Appendix

The appendix holds figures showing the current speed and direction of the complete sea trial. Each figure covers a calendar week and shows measurements from the Datawell ACM and the RDI ADCP (bin 21). In some figures, only the Datawell ACM is visible. This is because the RDI ADCP is undergoing maintenance at that time.

Week 1

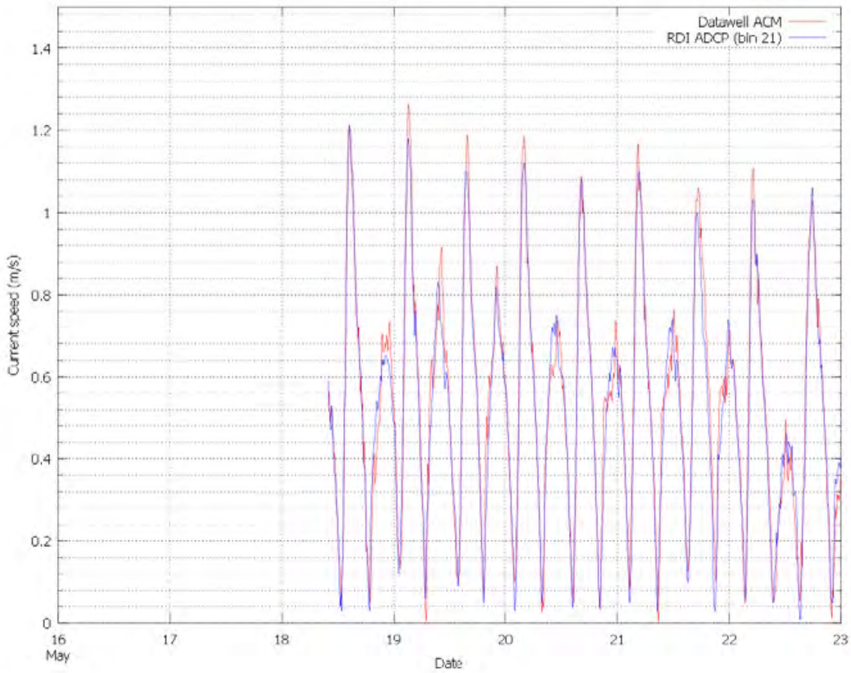


**Figure 18** Current speed as measured by the Datawell ACM and the RDI ADCP (bin 21).

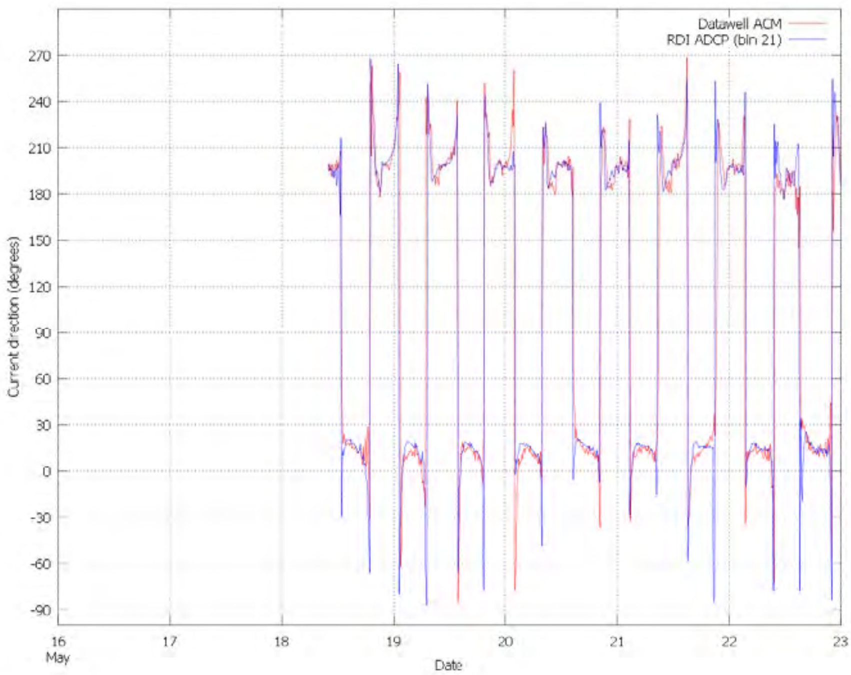


**Figure 19** Current direction as measured by the Datawell ACM and the RDI ADCP (bin 21).

Week 2

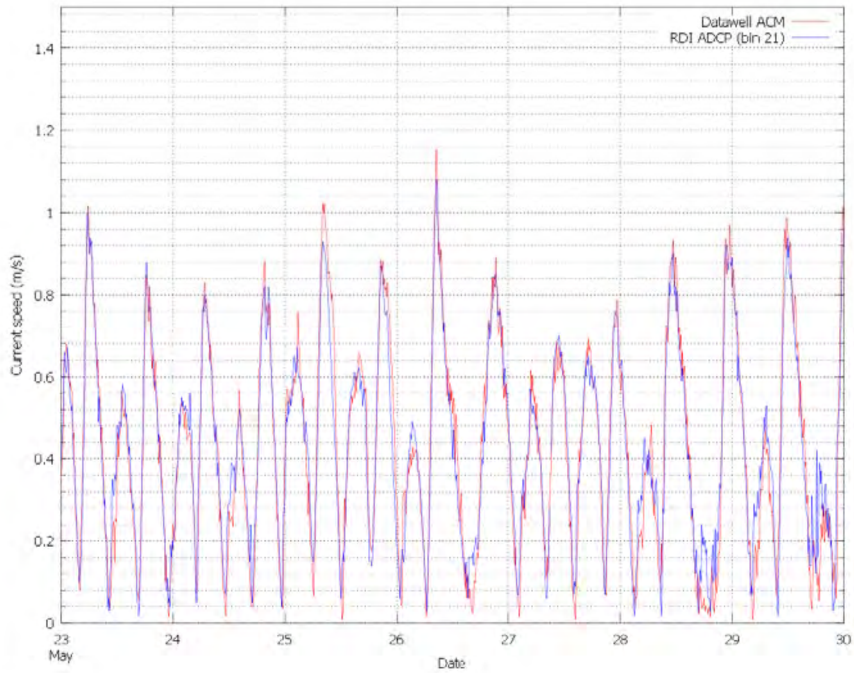


Figure 20 Current speed as measured by the Datawell ACM and the RDI ADCP (bin 21).

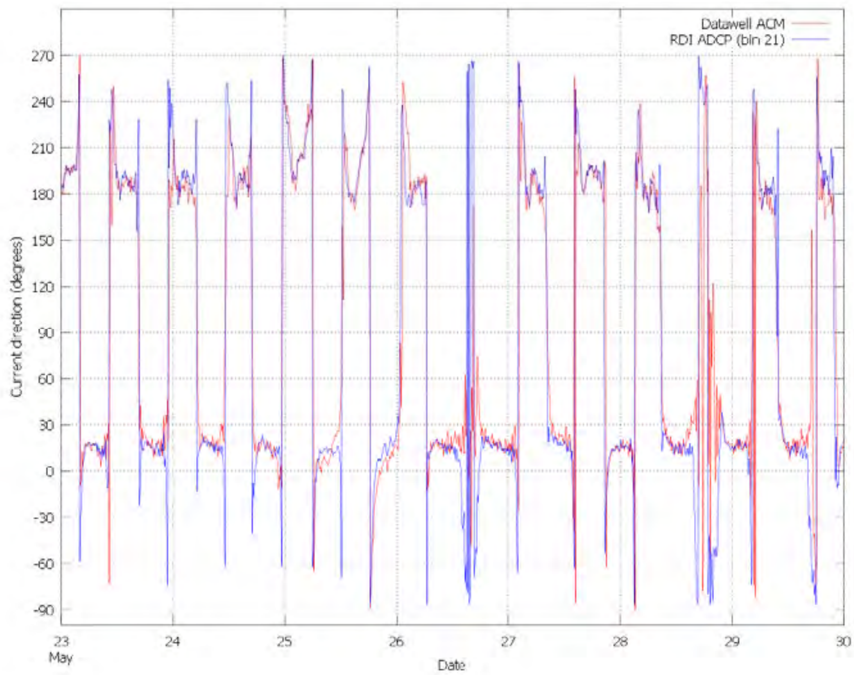


Figure 21 Current direction as measured by the Datawell ACM and the RDI ADCP (bin 21).

Week 3

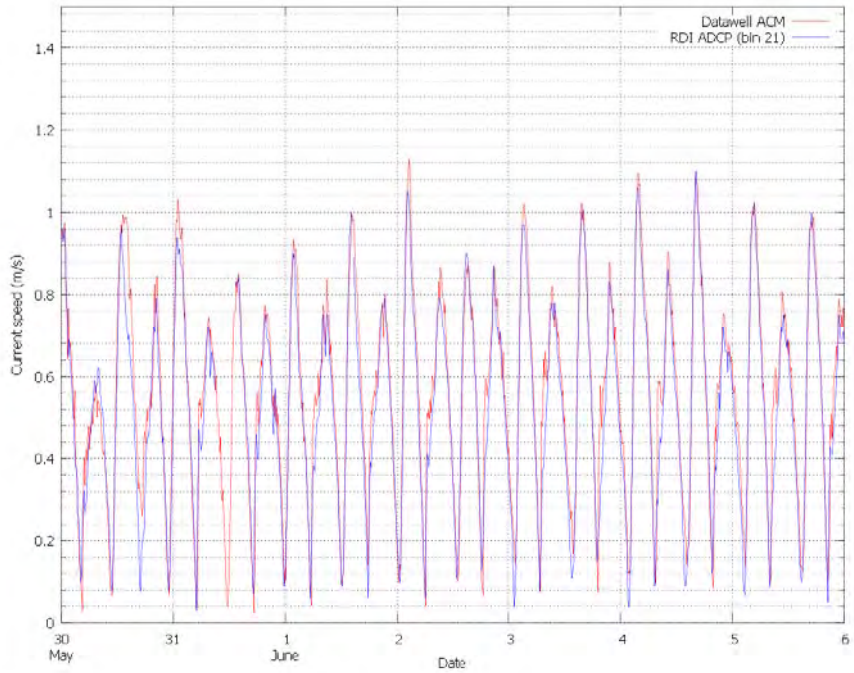


Figure 22 Current speed as measured by the Datawell ACM and the RDI ADCP (bin 21).

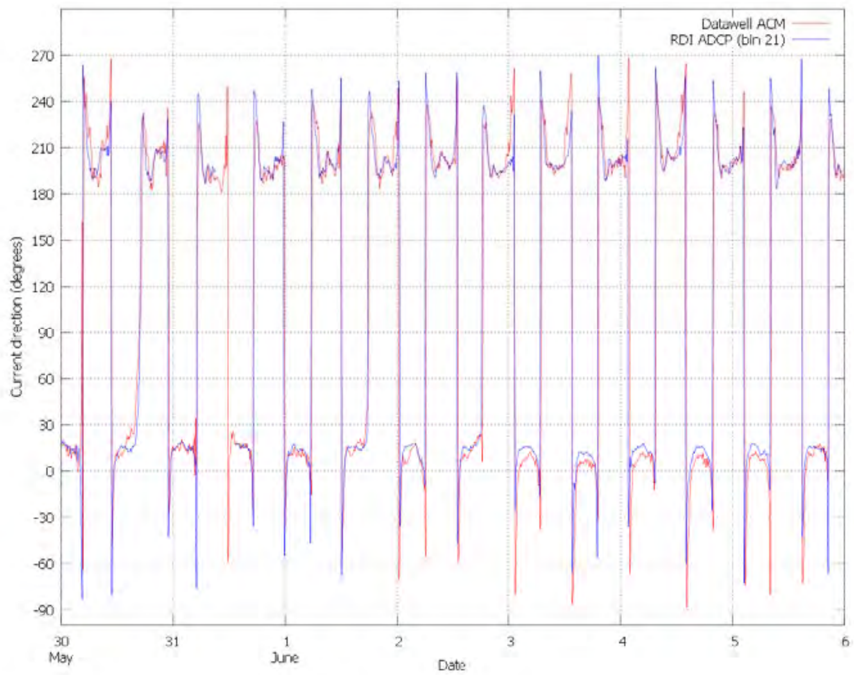


Figure 23 Current direction as measured by the Datawell ACM and the RDI ADCP (bin 21).

Week 4

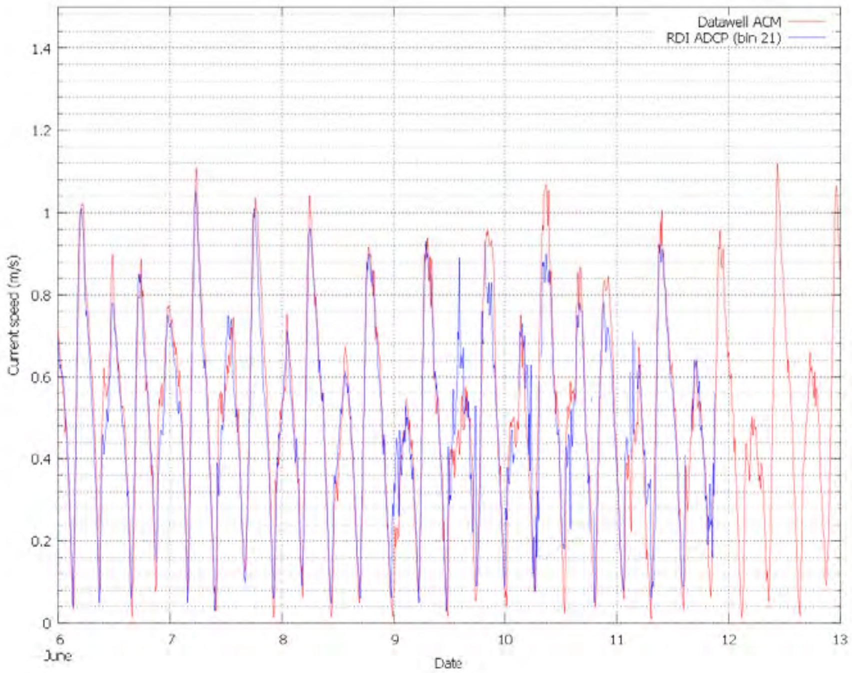


Figure 24 Current speed as measured by the Datawell ACM and the RDI ADCP (bin 21).

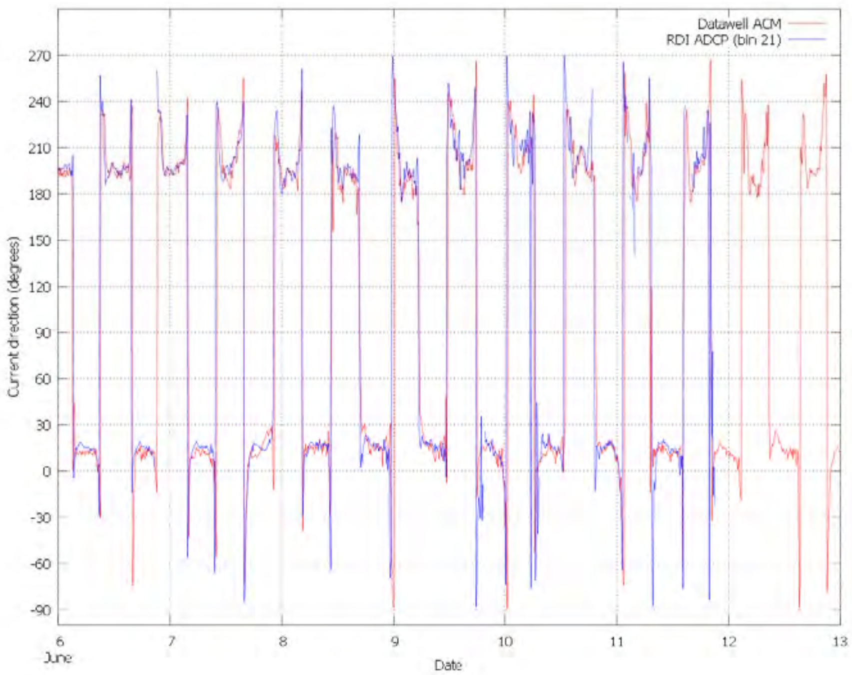


Figure 25 Current direction as measured by the Datawell ACM and the RDI ADCP (bin 21).

Week 5

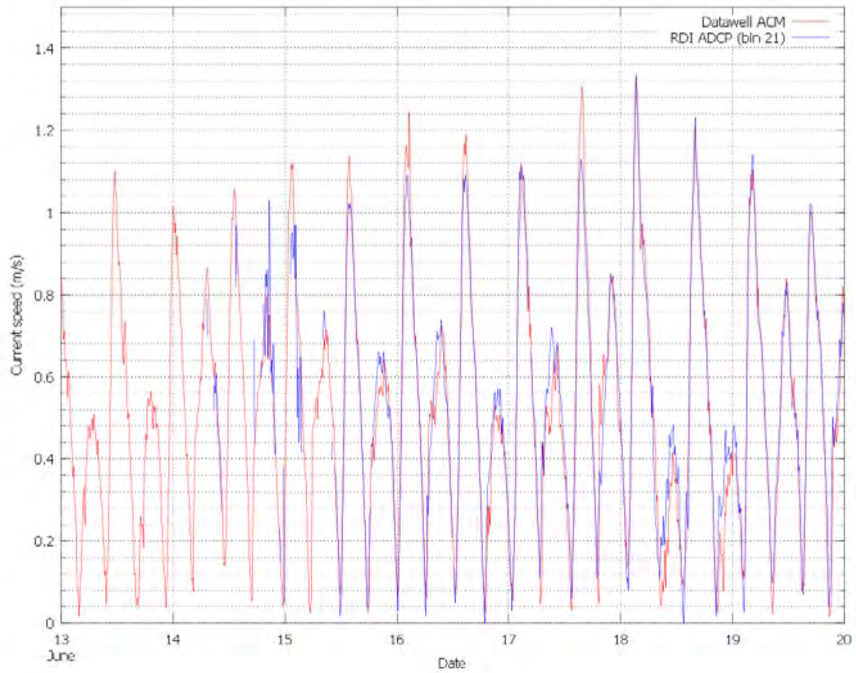


Figure 26 Current speed as measured by the Datawell ACM and the RDI ADCP (bin 21).

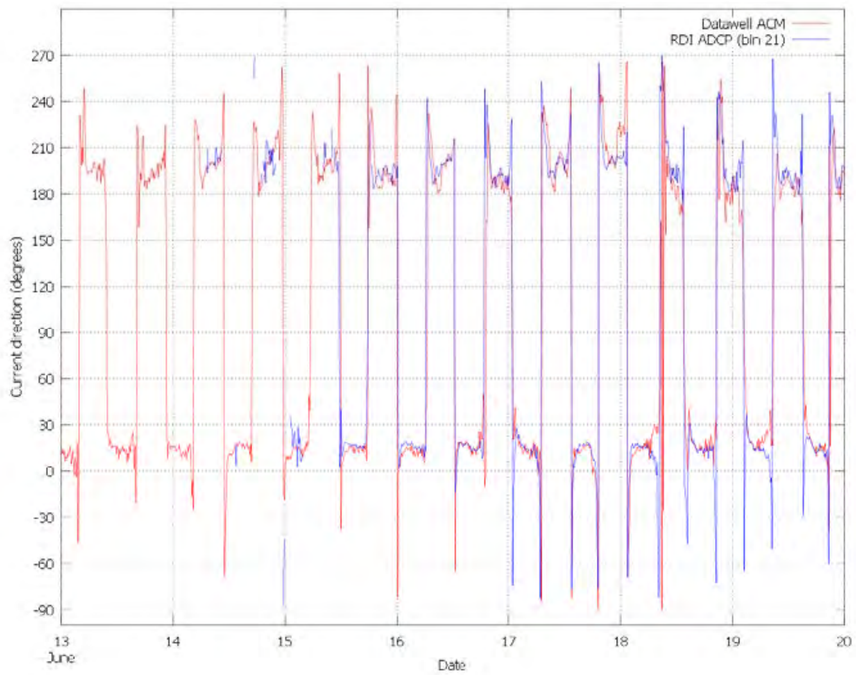


Figure 27 Current direction as measured by the Datawell ACM and the RDI ADCP (bin 21).

Week 6

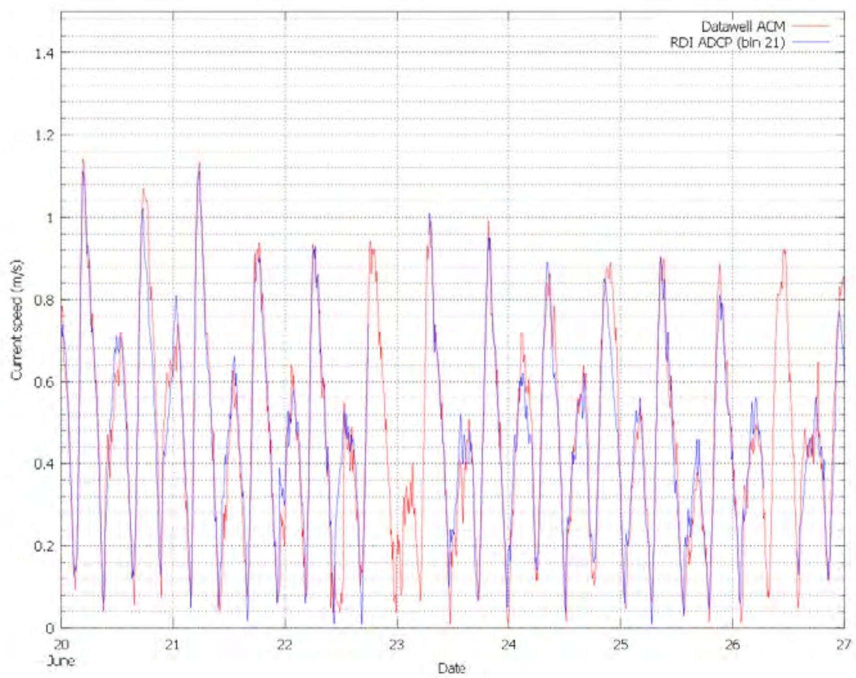


Figure 28 Current speed as measured by the Datawell ACM and the RDI ADCP (bin 21).

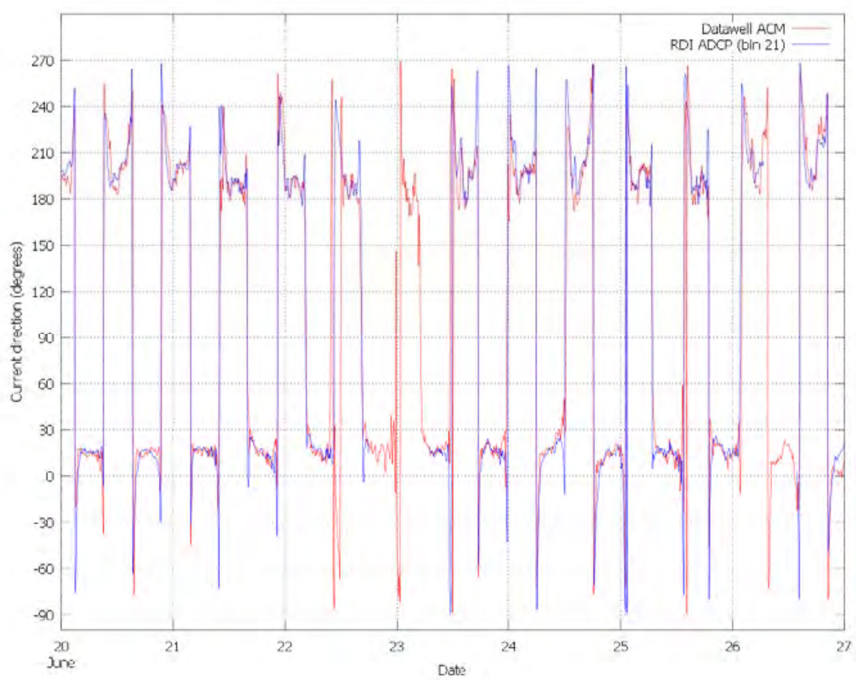


Figure 29 Current direction as measured by the Datawell ACM and the RDI ADCP (bin 21).

Week 7

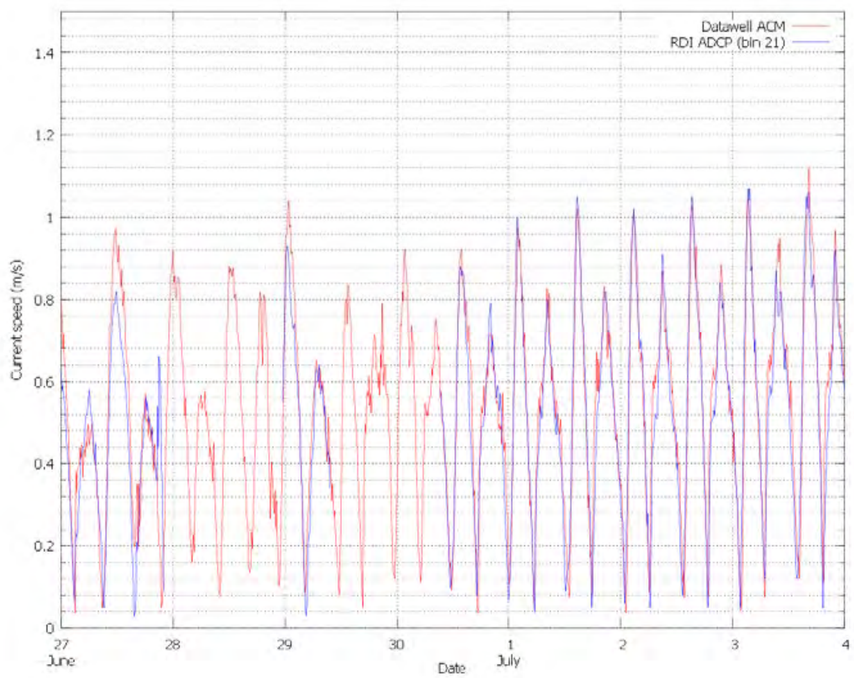


Figure 30 Current speed as measured by the Datawell ACM and the RDI ADCP (bin 21).

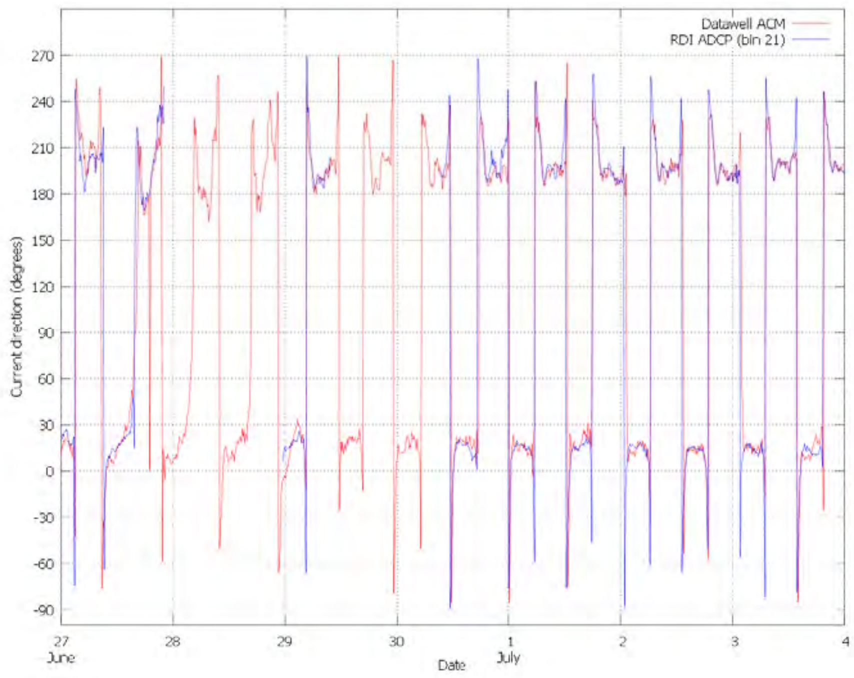


Figure 31 Current direction as measured by the Datawell ACM and the RDI ADCP (bin 21).

Week 8

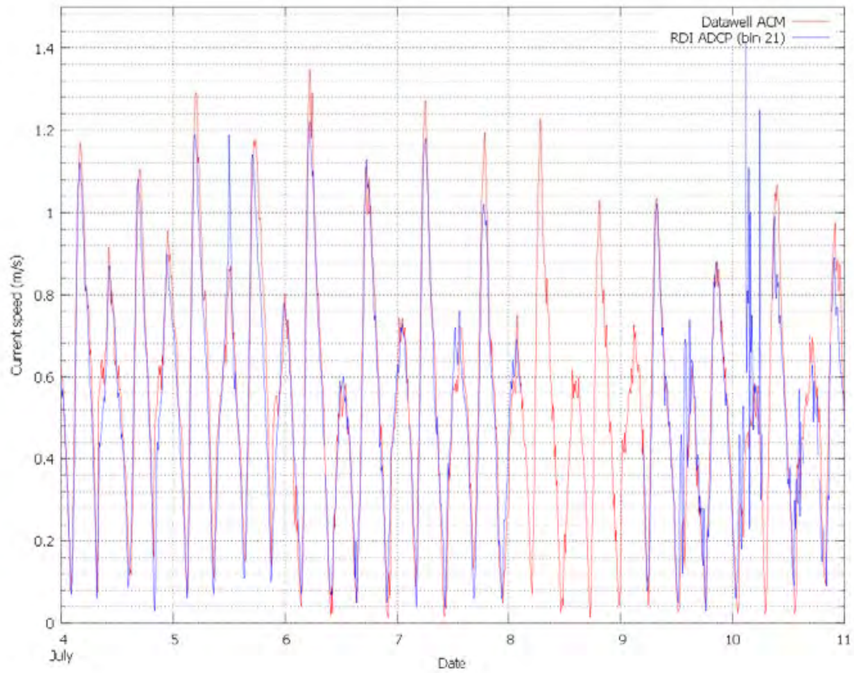


Figure 32 Current speed as measured by the Datawell ACM and the RDI ADCP (bin 21).

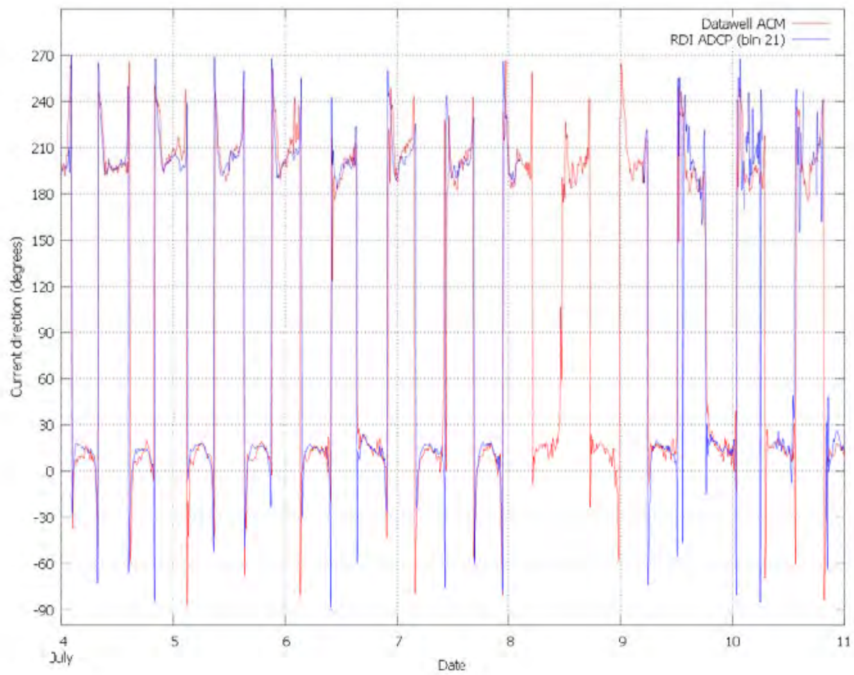


Figure 33 Current direction as measured by the Datawell ACM and the RDI ADCP (bin 21).

Week 9

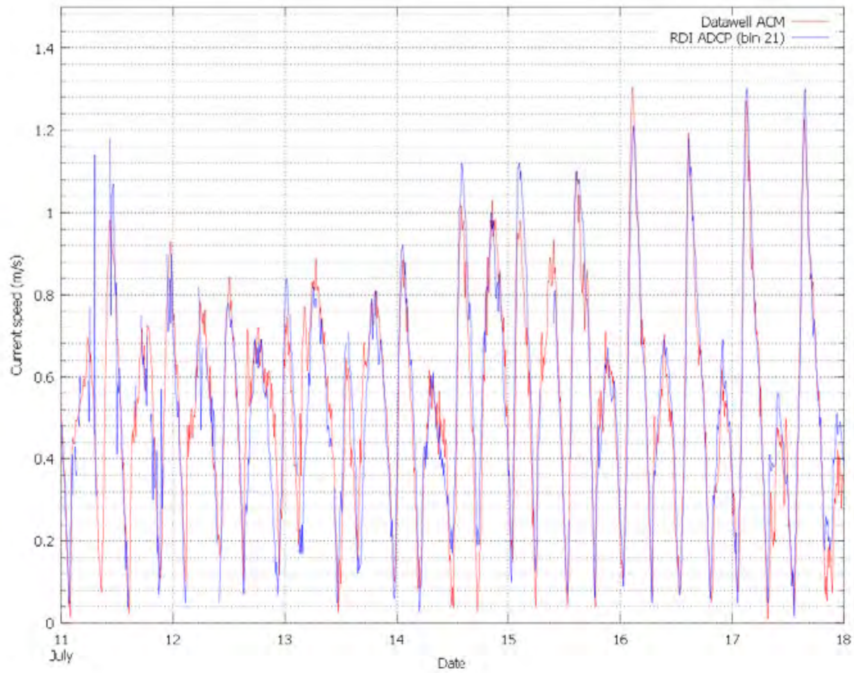


Figure 34 Current speed as measured by the Datawell ACM and the RDI ADCP (bin 21).

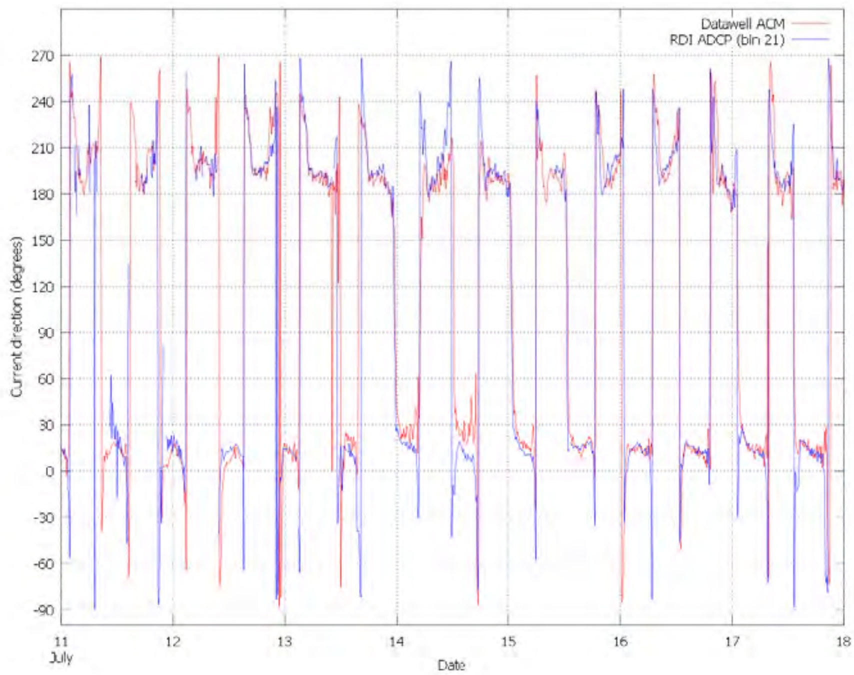


Figure 35 Current direction as measured by the Datawell ACM and the RDI ADCP (bin 21).

Week 10

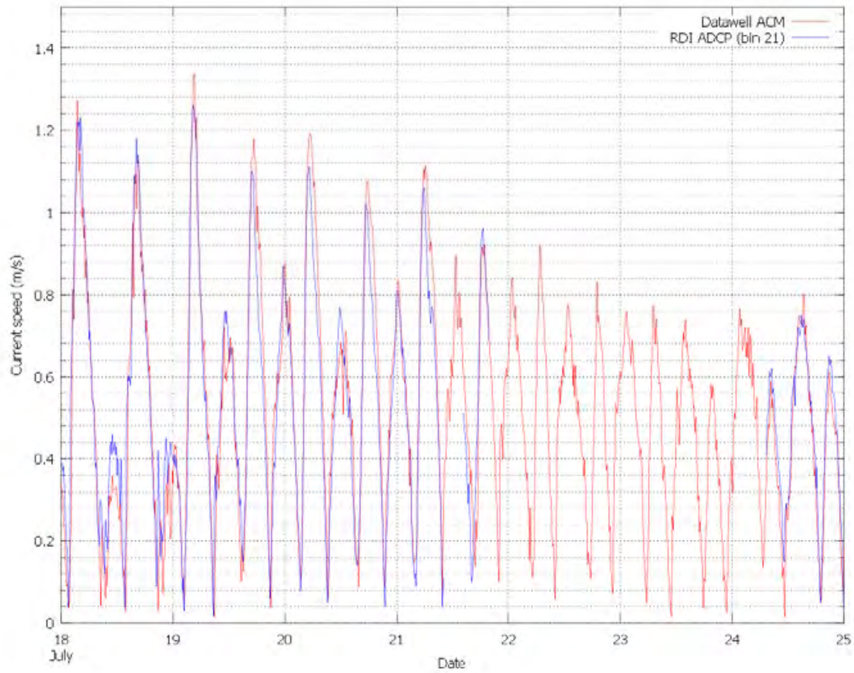


Figure 36 Current speed as measured by the Datawell ACM and the RDI ADCP (bin 21).

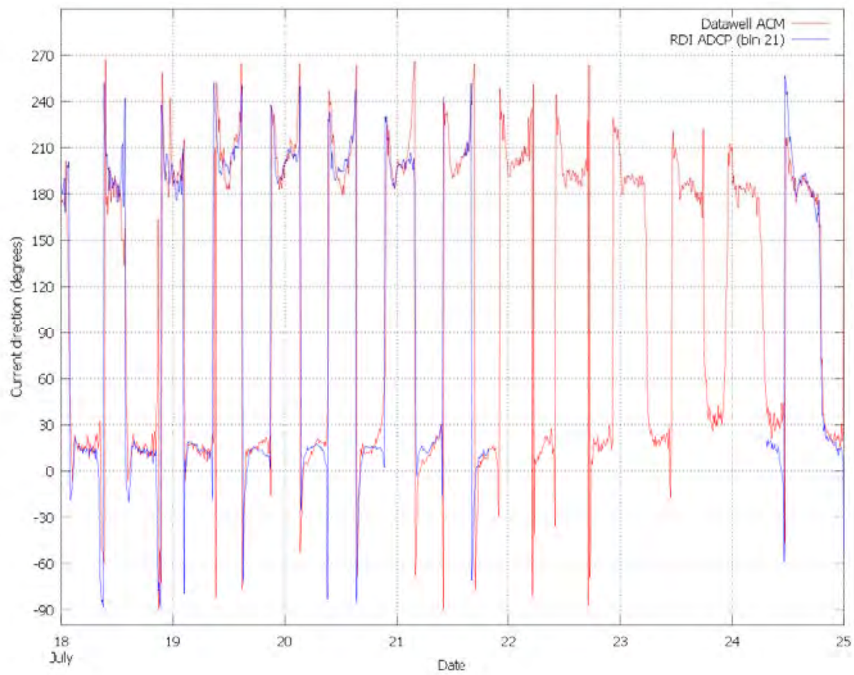


Figure 37 Current direction as measured by the Datawell ACM and the RDI ADCP (bin 21).

Week 11

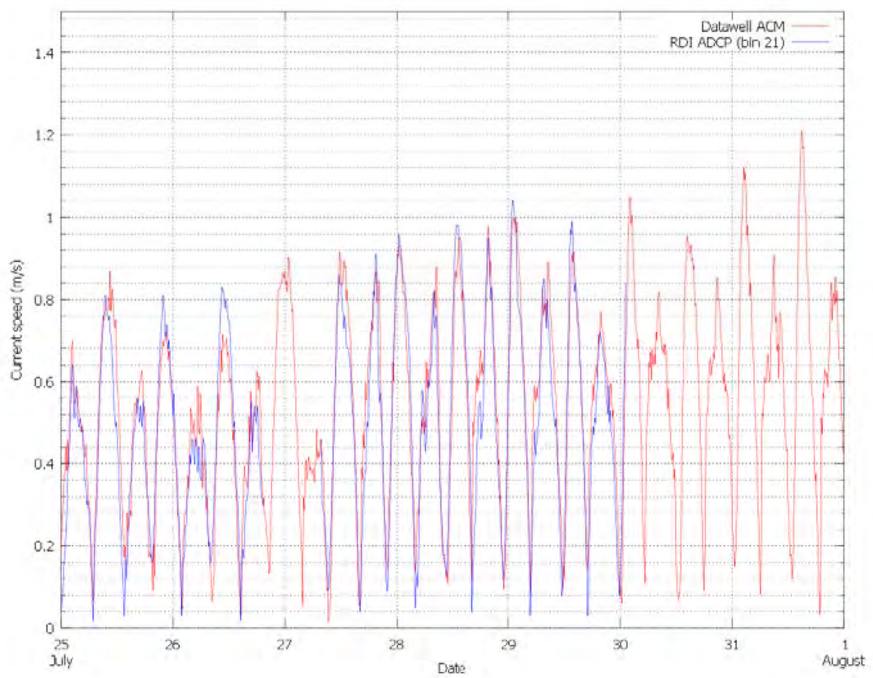


**Figure 38** Current speed as measured by the Datawell ACM and the RDI ADCP (bin 21).

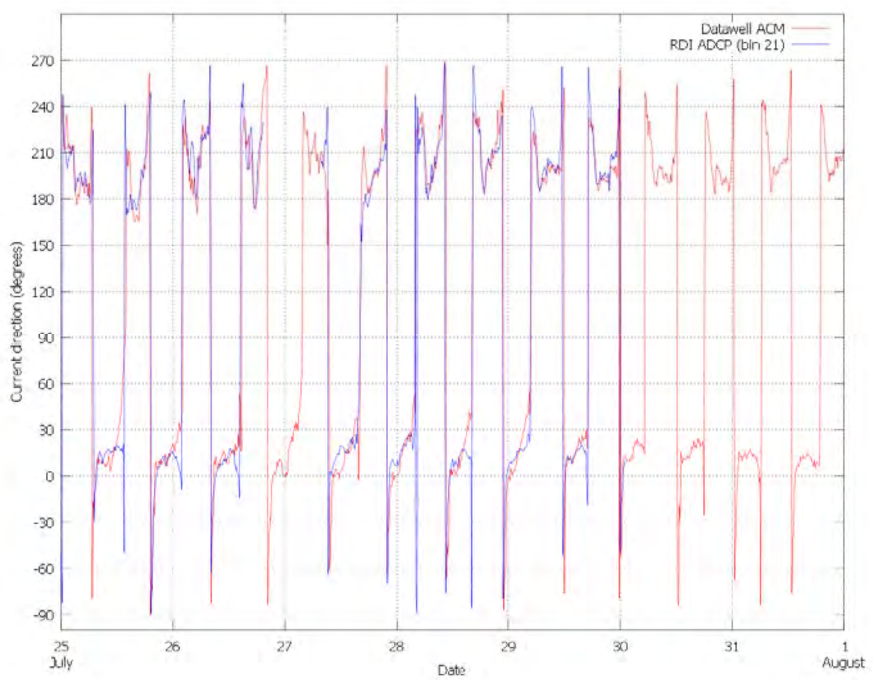


**Figure 39** Current direction as measured by the Datawell ACM and the RDI ADCP (bin 21).

Week 12

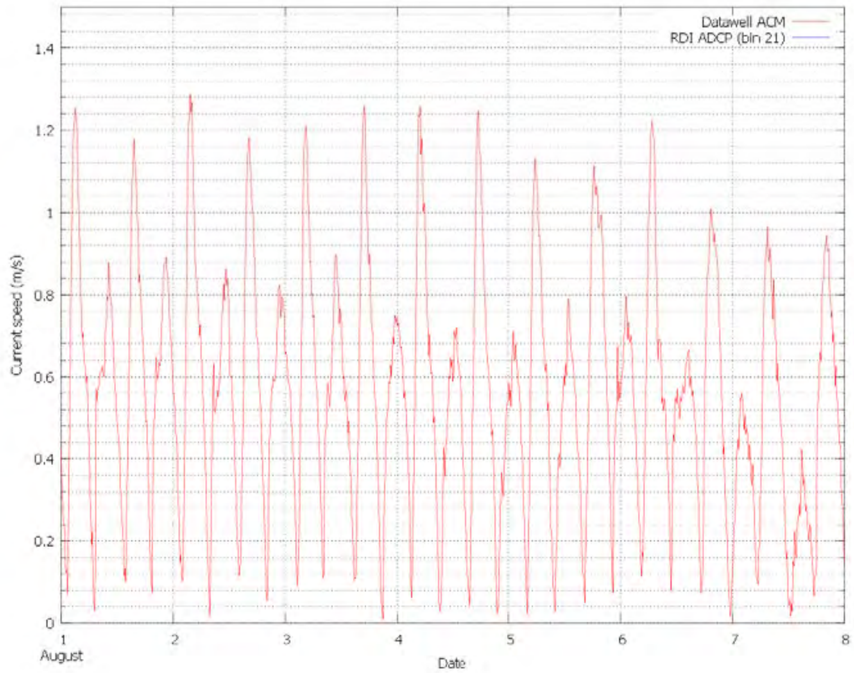


Figure 40 Current speed as measured by the Datawell ACM and the RDI ADCP (bin 21).

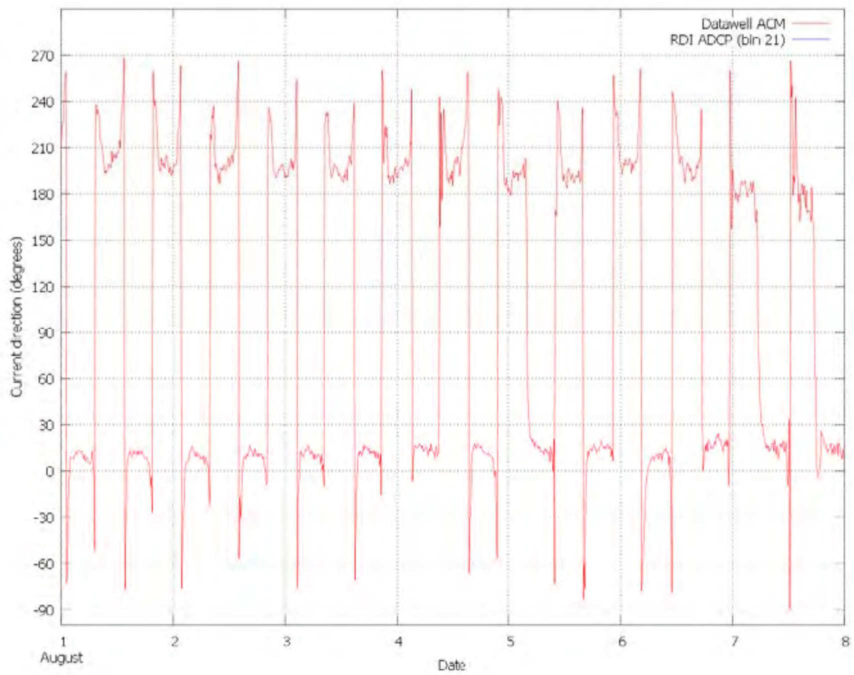


Figure 41 Current direction as measured by the Datawell ACM and the RDI ADCP (bin 21).

Week 13

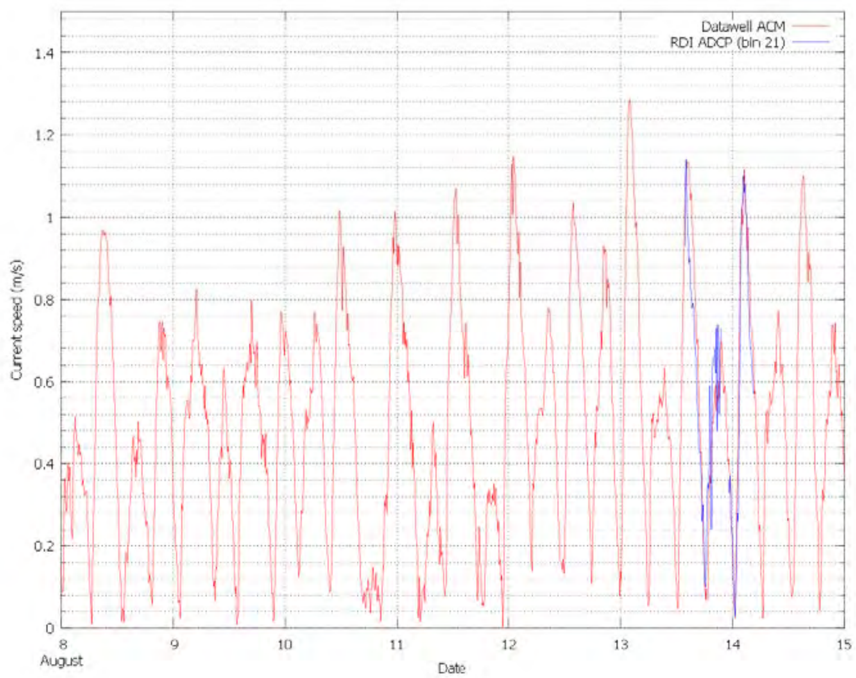


Figure 42 Current speed as measured by the Datawell ACM and the RDI ADCP (bin 21).

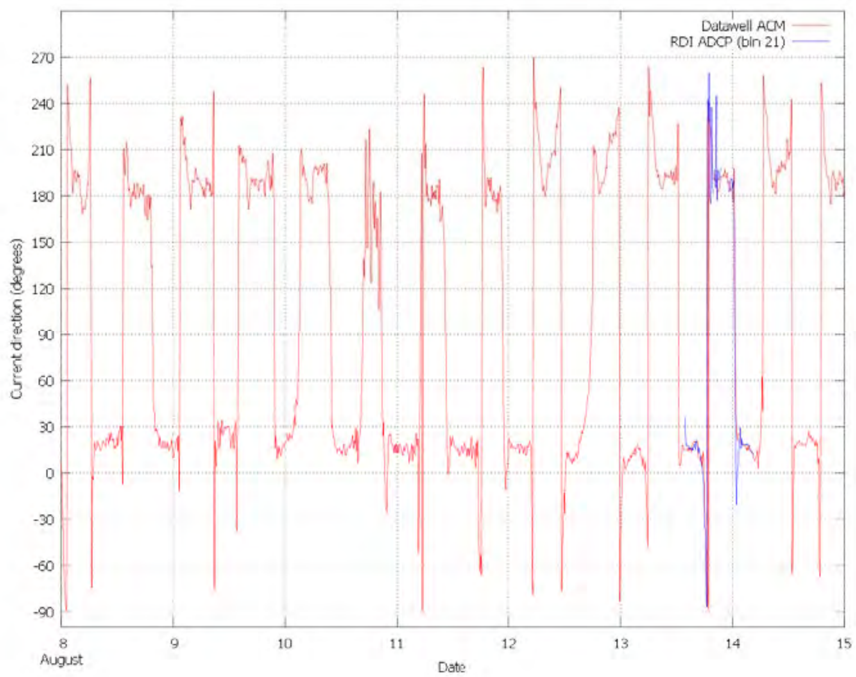


Figure 43 Current direction as measured by the Datawell ACM and the RDI ADCP (bin 21).

Week 14

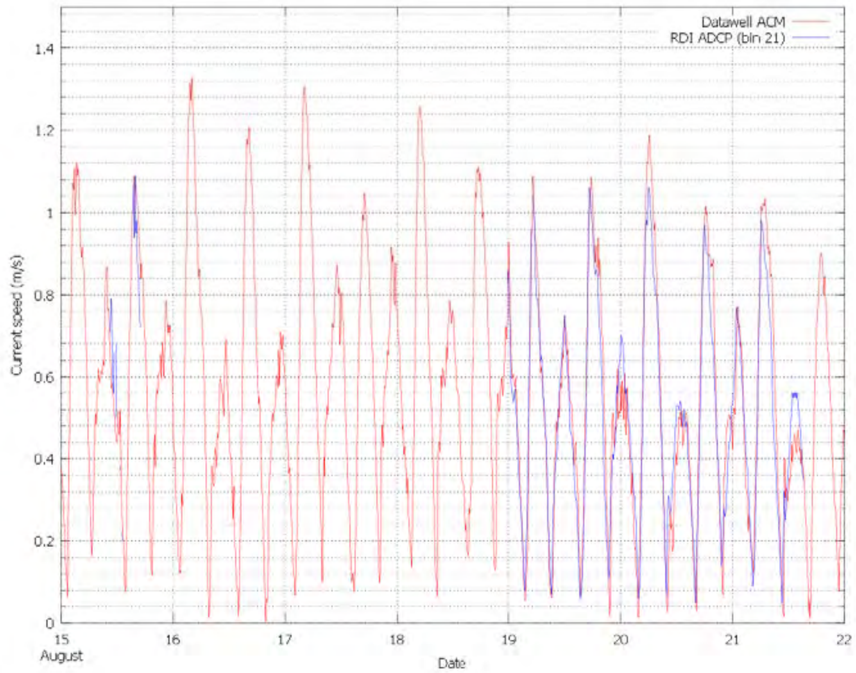


**Figure 44** Current speed as measured by the Datawell ACM and the RDI ADCP (bin 21).

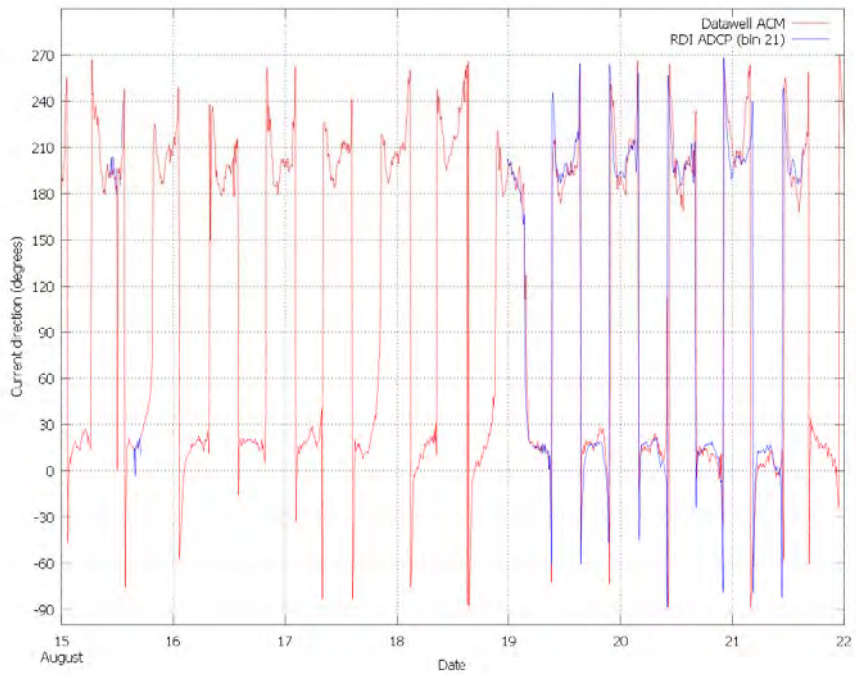


**Figure 45** Current direction as measured by the Datawell ACM and the RDI ADCP (bin 21).

Week 15

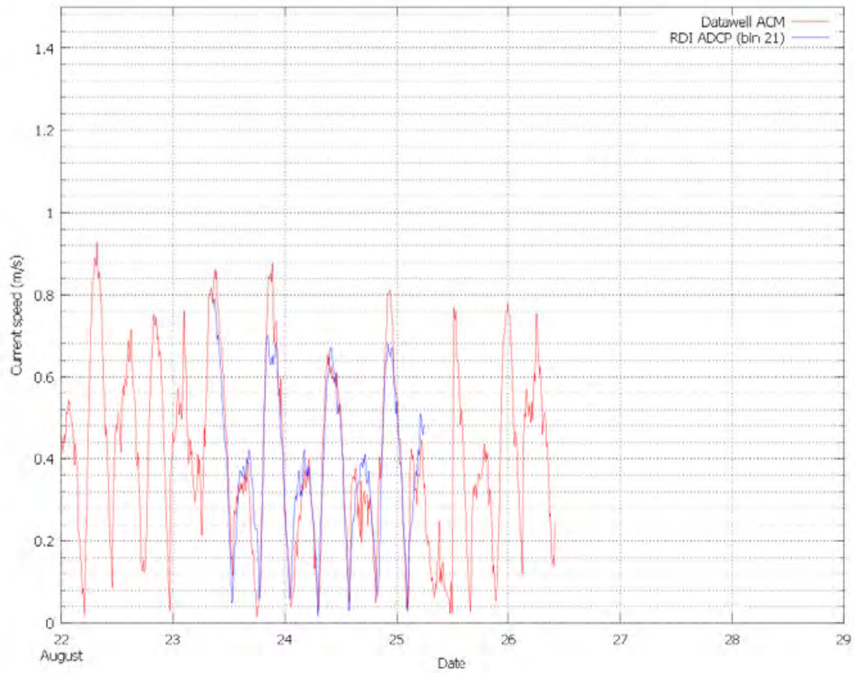


Figure 46 Current speed as measured by the Datawell ACM and the RDI ADCP (bin 21).

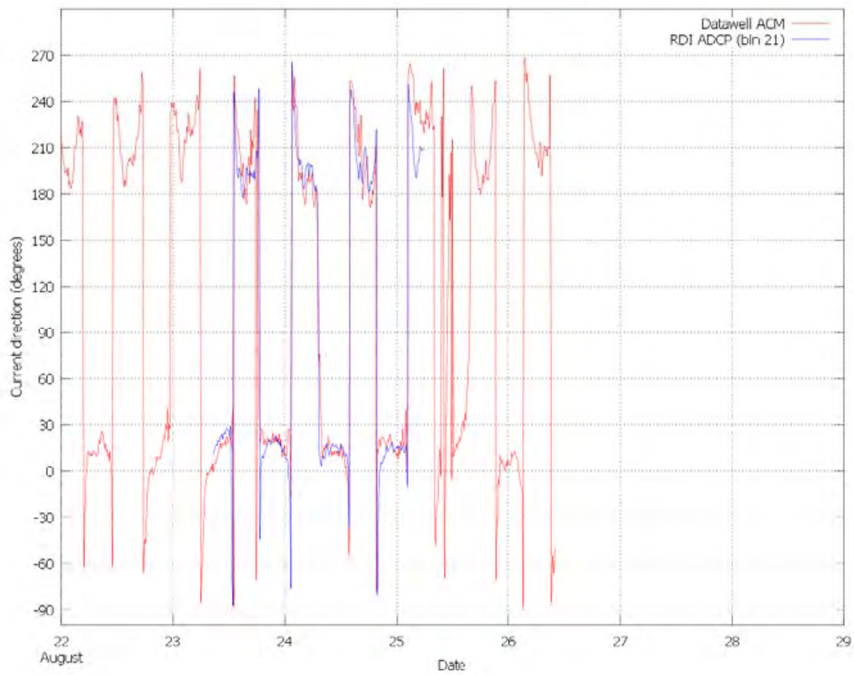


Figure 47 Current direction as measured by the Datawell ACM and the RDI ADCP (bin 21).

# A comparative report on the DWR MkIII and DWR4 data

During the development of the DWR4, the successor of the DWR MkIII with higher sampling frequency and improved data processing, many long and short term buoy deployments were conducted off the shore at Ymuiden, The Netherlands. A test from November 29 to December 22, 2011, profited from a large variety of meteorological conditions and sea states. Periods of calm were interspersed with rough and ferocious storms. During the test period, the significant wave height actually varied between 1 and 5.5 m, which are extreme values in 15 m water depth. The data of this test buoy that included both MkIII functionality and DWR4 functionality is used to compare both processing schemes. The results of this comparison are presented and explained in this report. It is shown that both processing schemes perform well and the minor differences of the results can be attributed to the higher sample frequency.

## Scheme differences

In the new DWR4 data processing, a number of changes have been introduced.

- Foremost is the doubling of the sampling frequency, from 1.28 Hz in the MkIII to 2.56 Hz in the DWR4. This sampling frequency is the rate at which the buoy outputs the displacement data, the socalled ‘external’ sample rate. The primordial acceleration is sampled at a higher rate, and this ‘internal’ sampling frequency is increased from 3.84 Hz in the MkIII to 5.12 Hz in the DWR4.
- Secondly, the resolution of the displacement data has been changed through the use of a arcsinh (inverse hyperbolic sine) representation of numbers. This representation resembles a floating point notation of 12 bits having a 3-bit exponent. Both have an essentially logarithmic value distribution. Thus millimetre resolution for small values is realised, rising to 4 cm resolution at the maximal displacement of 20 metres.
- For the spectral analysis, both the MkIII and the DWR4 rely on Welch’s method that estimates the power spectrum by calculating the periodogram over windowed data segments using the Fast Fourier Transform. The difference here is the use of the Hann window in the DWR4, opposite to a Tukey window with $\alpha = 0.25$ in the MkIII. Also, the data segments in the DWR4 overlap (50%), whereas in the MkIII they do not. As a result, the number of segments in a 30 minutes record increases from 8 in the MkIII, to 17 in the DWR4, and this increase results in a smaller variance of the DWR4 spectrum.
- The length of a data segment expressed in seconds is equal in both schemes. Expressed in number of datapoints, a DWR4 segment is twice as long as a MkIII segment. As a result, the frequency step in the spectrum remains the same, 0.005 Hz for MkIII and DWR4 alike, but the frequency interval increases, from 0.025 – 0.58 Hz in the MkIII to 0.025 – 1.00 Hz in the DWR4, virtually a doubling of the range.
- Until now the analysis of the wave data in terms of zero-upcross waves was not implemented in the buoy firmware, but was left for the post-processing. In the DWR4 however, some basic zero-upcross wave analysis is implemented, specifically the one-loop calculations that can be performed “on the fly” and do not require data storage or sorting. These include $H_{max}$, the maximal wave height, and an estimator of $H_s$, the significant wave height, based on the rms (root-mean-square) value of the upcross wave heights: $H_s = H_{rms}\sqrt{2}$. The latter parameter serves as an alternative for $H_{1/3}$.
- Finally, a rudimentary level of quality control is added in the DWR4 scheme. The rare events that pitch or roll angles exceed 89°, or that accelerations exceed 1 g (standard gravity), are flagged, and segments containing such exceptions are precautionarily excluded from the spectral calculations. It is emphasized here that the occurrence of a flag does not imply an error, nor does the absence of a flag warrant a correct measurement. A flag is merely indicative of a sensor having got near the limits of its range.

### Spectral parameters

An easy, yet significant test is the comparison of the main spectral parameters: the significant wave height ($H_{m0}$), the mean period ($T_1$), the zero-upcross period ($T_z$) and the crest period ($T_c$). Because of the wider frequency interval for the DWR4, we expect the spectral parameters of the new buoy to have slightly lower values than their MkIII counterparts. The effect will be strongest in the crest period that depends on the 4$^{th}$ spectral moment, while hardly noticeable in the



Datawell BV
Zomerluststraat 4
2012 LM Haarlem
The Netherlands

T +31 23 531 60 53
F +31 23 531 19 86
E sales@datawell.nl
W www.datawell.nl

significant wave height depending on the 0th moment only. The spectral moments are integrals of the power spectral density on the full frequency interval. In principle the upper limit is infinity, in reality it is finite. Thus the values of the moments, and of the spectral parameters derived from them, depend on the upper frequency limit that has been increased from 0.58 Hz to 1.0 Hz.

In order to make a fair comparison between the schemes, we therefore introduce two sets of parameter values in the DWR4: one for the full range of 0.025 – 1.0 Hz and indicated by the abbreviation FR, and one for the mid range of 0.025 – 0.58 Hz, indicated by MR. We thus expect the MkIII numbers to be slightly greater than the DWR4 (FR) numbers, and much more close to the DWR4 (MR) numbers.

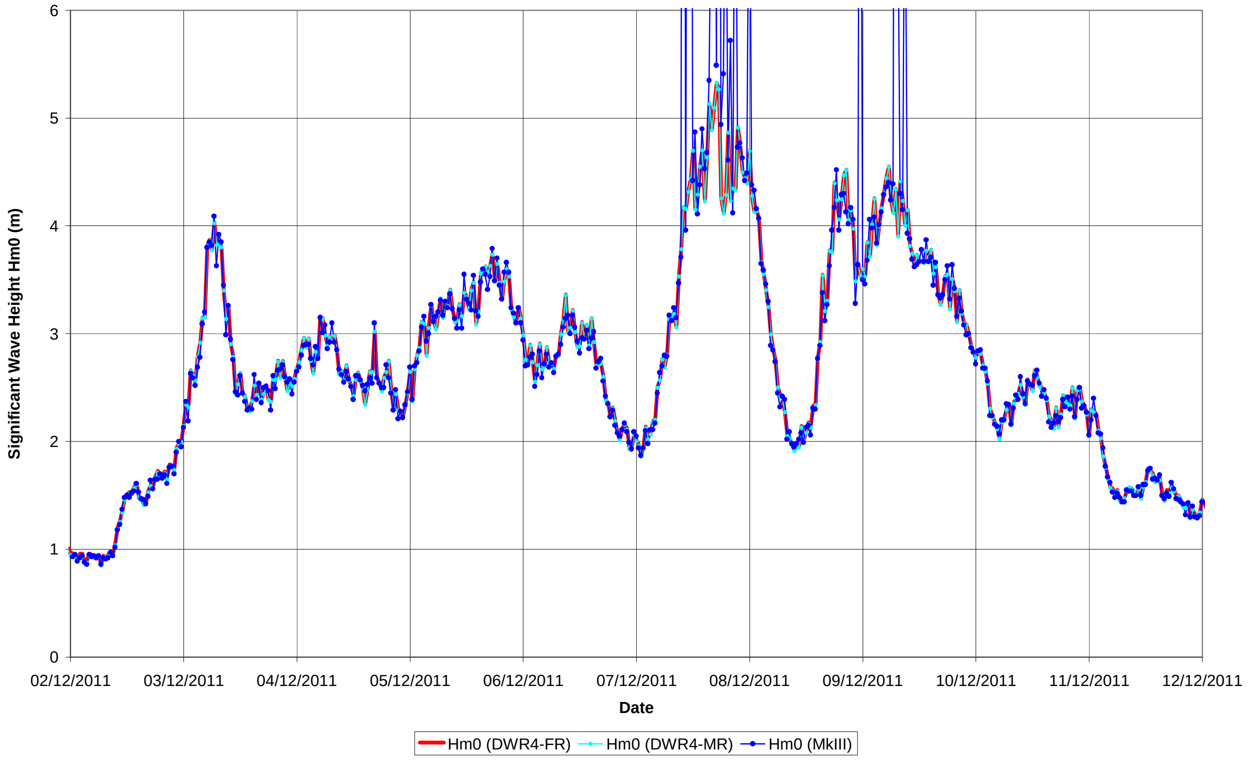


**Fig 1**. Comparison of the significant wave height $H_{m0}$

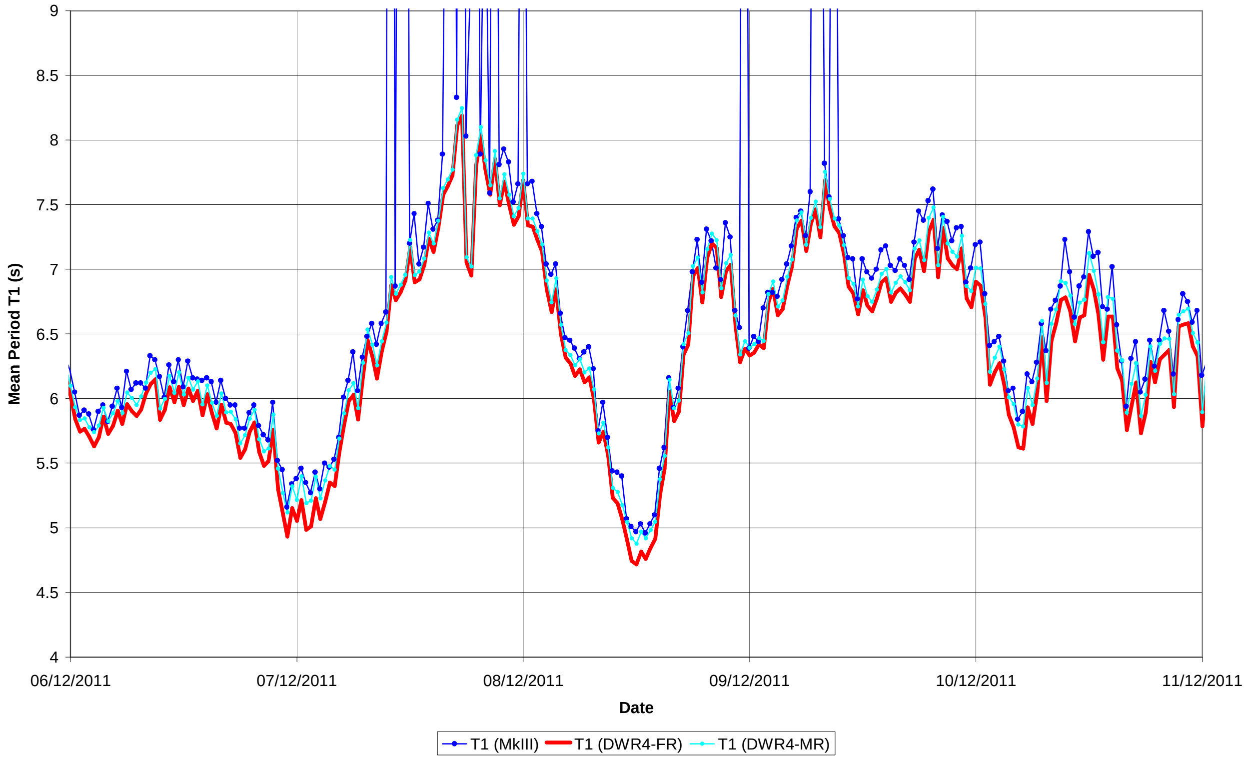


**Fig 2**. Comparison of the mean period $T_1$. Only five days are shown for better visualising of differences.

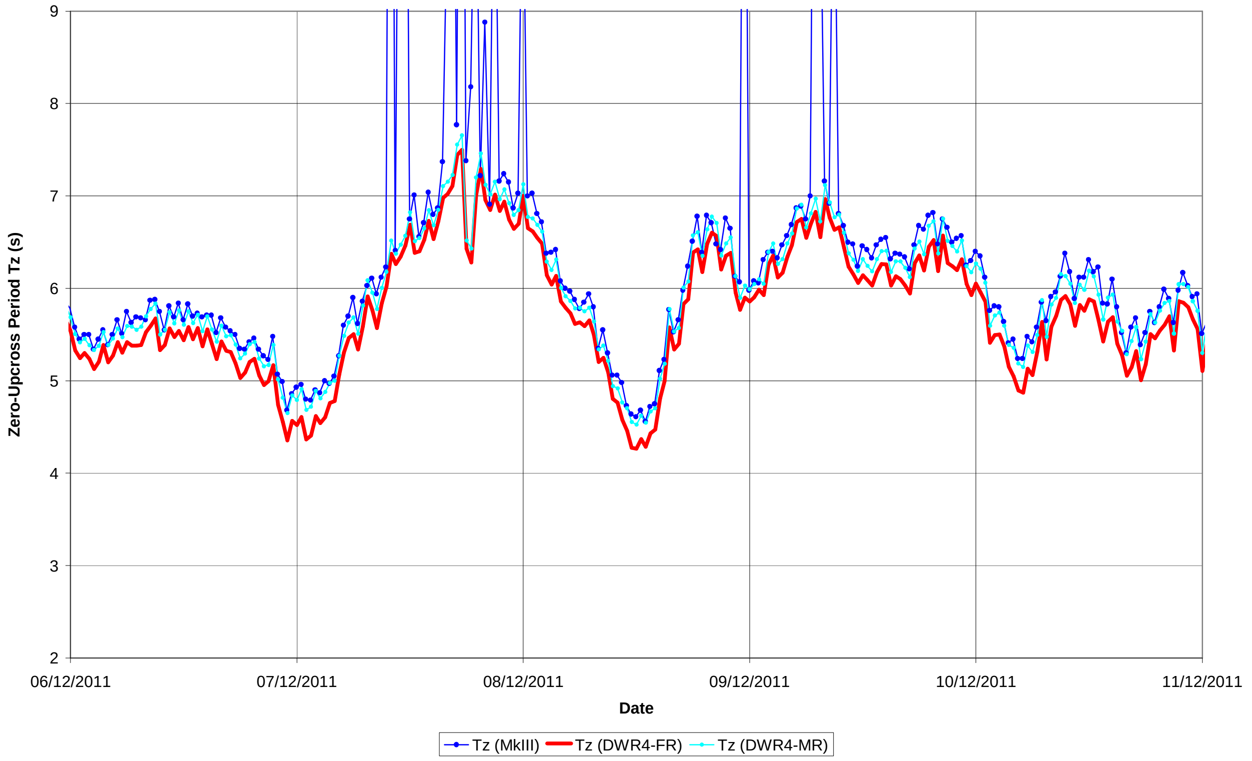


**Fig 3**. Comparison of the zero-upcross period $T_z$

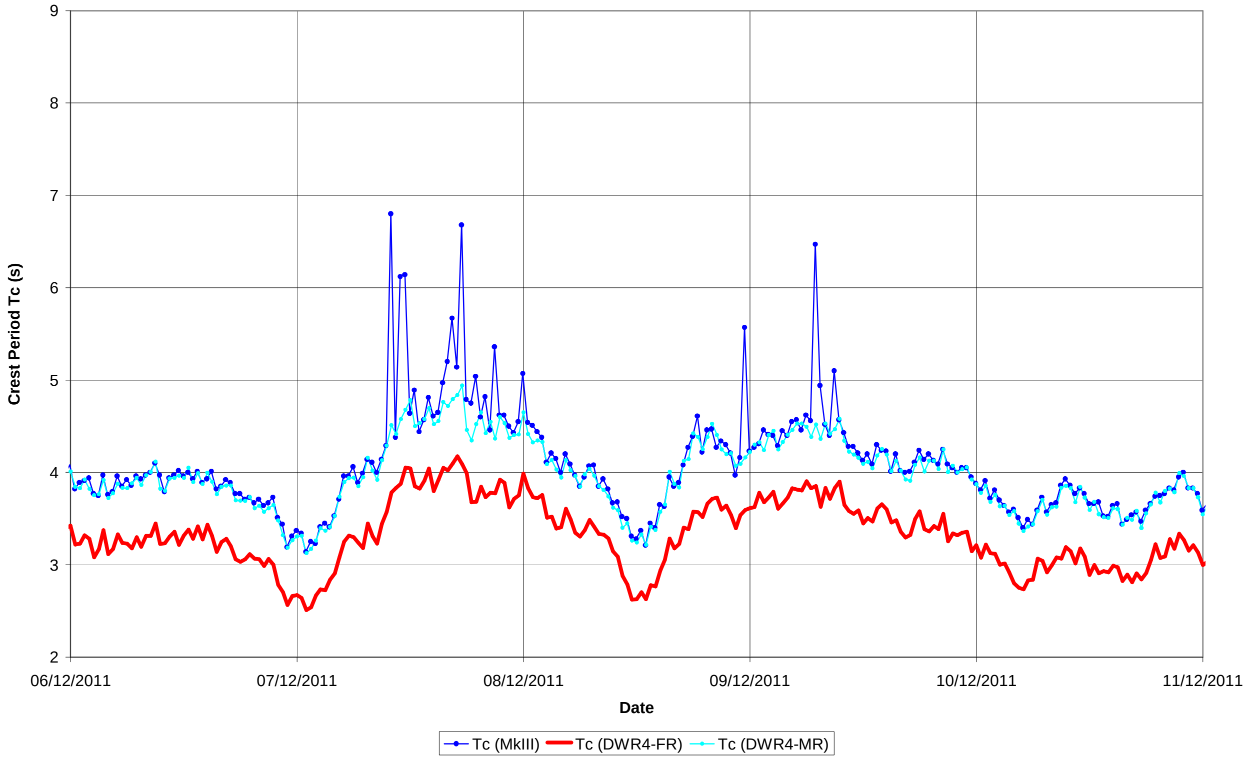


**Fig 4**. Comparison of the crest period $T_c$

In the figures above, the MkIII values are plotted as blue dots on a solid blue line. The DWR4 (FR) values are red, the DWR4 (MR) values are cyan. It is indeed seen that the impact of the upper frequency limit increases from Hm0 to Tc, and that the MkIII values agree well with the DWR4 (MR) values on the smaller frequency interval, both being consistently higher than the DWR4 (FR) values on the wider frequency interval.
A remark on the outliers in the plots is due here. These outliers all occurred during the two storms of 7 and 9 December, 2011, when the $H_{m0}$ measured over 4 m, exceptional values in 15 m deep water. They do not signal malfunctioning of the buoy, nor any errors in the processing of the measurements. Rather these stray values show that during these storms the buoy experienced forces that did not result from normal orbital wave motion but were exerted by large breaking waves, probably of the plunging type. That both DWR4 curves - MR and FR - show no outliers is due to the quality control in this scheme that was described in the previous section.
It must be realised that this first test actually comprises most of the data processing: all heave information, the segmentation and windowing, the exact shape of the spectrum etc. This first comparison regarding the spectral parameters is hence a highly relevant test.
The conclusion must be that the new DWR4 scheme produces the same results as the MkIII if the traditional frequency interval is used. If the new, wider frequency interval is used, the parameter values are expectedly lower, an effect that is small in the $H_{m0}$ and large in the $T_c$, in accordance with the theory.

## Zero-upcross wave statistics

The DWR4 outputs some statistical parameters based on the analysis of zero-upcross waves. Only those parameters are output that can be calculated in one loop, "on the fly", without storage or sorting of intermediate results. These include the highest wave Hmax, and the period of the highest wave $T(H_{max})$, the longest wave $T_{max}$, and the height of the longest wave $H(T_{max})$, the average wave height $H_{avg}$ and the average wave period $T_{avg}$, the number of upcross waves $N_w$, and the number of crests (maxima) $N_c$. In addition, the rms (root-mean-square) of the wave heights ($H_{rms}$) is used to obtain an estimator of the significant wave height $H_s = H_{rms}\sqrt{2}$.

The MkIII buoys do not output any statistical parameters. However some of the parameters are available in post-processing. Thus we can compare the two schemes with respect to $H_{max}$ and $T(H_{max})$, $H_{avg}$ and $T_{avg}$, $N_w$ and $N_c$. Also, we can compare the above mentioned $H_{rms}\sqrt{2}$ to $H_{1/3}$, the average wave height of the highest one third of the waves, being the original definition of the significant wave height. It must be realised that this latter comparison is different in nature from the other. The two parameters, generated by to completely different algorithms, are only equal in value if the upcross waves obey a Rayleigh distribution. So strictly speaking, this comparison is a test of the “Rayleigh-ness” of the waves, rather than a comparison between the MkIII and the DWR4 results. Since however the Rayleigh assumption is so generally valid, agreement between $H_{1/3}$ and $H_{rms}\sqrt{2}$ is yet considered indirect proof of concordance of the two schemes.
A number of parameters stay outside the comparison: the MkIII parameters $H_{1/10}$ and $T(H_{1/10})$, the average wave height of the highest one tenth of the waves and the associated period, and also $T(H_{1/3})$, of obvious definition, have no DWR4 counterparts, since they cannot be calculated on the fly. On the other hand, the DWR4 parameters $T_{max}$ and $H(T_{max})$ are new and without MkIII equivalents: these parameters are actually borrowed from the analysis method as implemented by one of our major customers. Their introduction is inspired by our wish to coordinate our methods of data analysis. Inclusion of these parameters in the plots below is merely illustrational.
In Figure 5, the upcross height parameters are plotted, the DWR4 values as solid lines, the MkIII values as dots. We find an excellent agreement for all three heights: $H_{max}$, $H_{avg}$ and $H_s$ (given by $H_{1/3}$ in the MkIII and by $H_{rms}\sqrt{2}$ in the DWR4). The time series of both $H_{avg}$ and $H_s$ show very smooth, and parallel, trends. In contrast, $H_{max}$ is much more fluctuating in time, and the concordance of the DWR4 and the MkIII is all the more remarkable. Figure 5 comprises just five days to reveal the finer details of the time series. In Figure 6 the complete time series are plotted, spanning a full month. The agreement is perfect, except for the storm events on 7 and 9 December, where wave heights greater than six metres were measured. Here the drawback of the upcross wave analysis becomes clear: the usefulness of its results depends crucially on the strictness of the data quality control. This however is not different between the two schemes, and only shows that the expert’s eye is indispensable for the correct assessment of wave-statistical results.
Figure 7 shows the wave periods, again for a short interval of five days, to not obscure the details. Good agreement is seen for the $T(H_{max})$, the wave period of the highest wave. For the average wave period we see concurrent trends, where the DWR4 values are systematically lower than those of the MkIII by 0.1 or 0.2 seconds. Another way of putting this is that the DWR4 registers slightly more waves than the MkIII (since $T_{avg}$ is simply the reciprocal of $N_w$).


Datawell BV
Zomerluststraat 4
2012 LM Haarlem
The Netherlands

T +31 23 531 60 53
F +31 23 531 19 86
E sales@datawell.nl
W www.datawell.nl

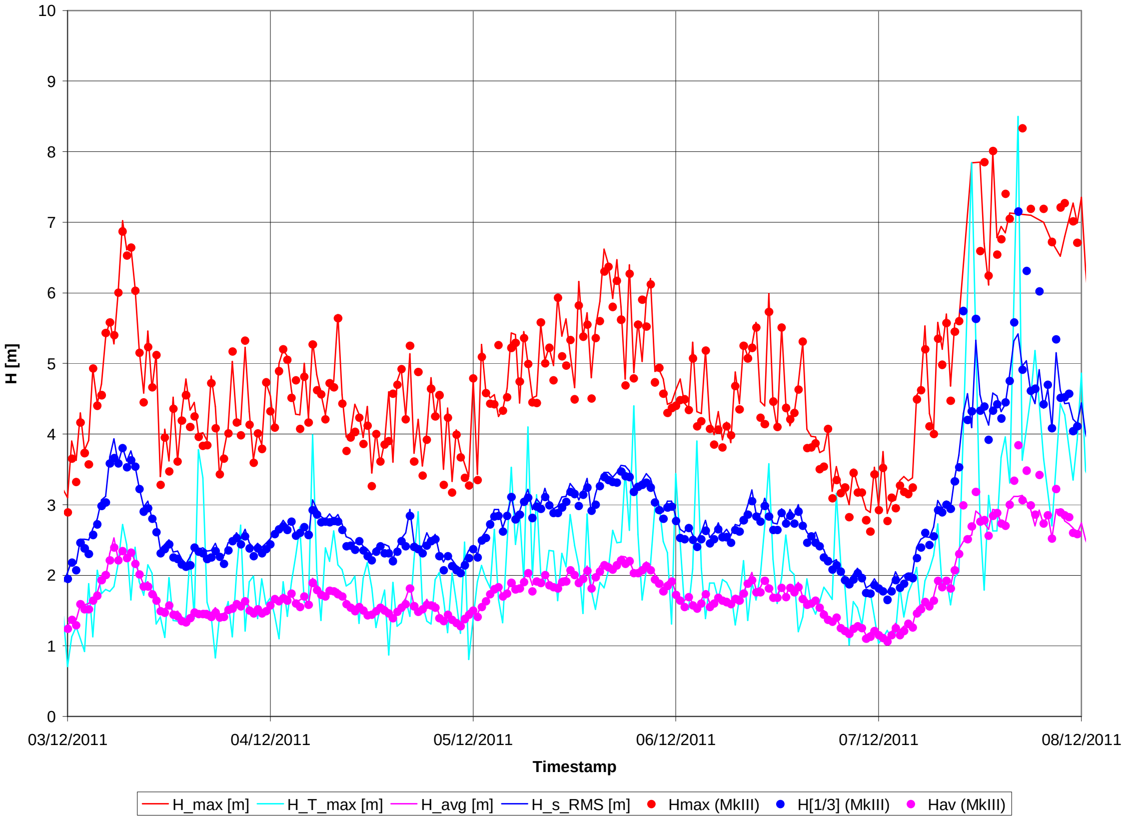


**Fig 5**. Wave height parameters in the zero-upcross wave analysis (detail)

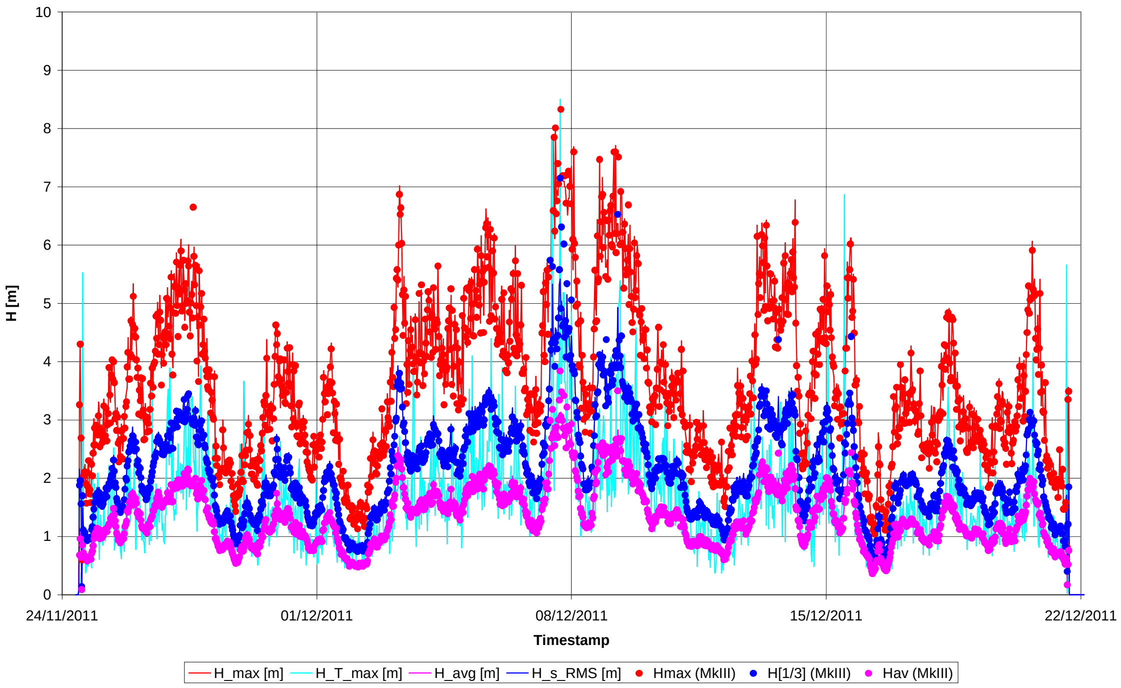


**Fig 6**. Wave height parameters in the zero-upcross wave analysis

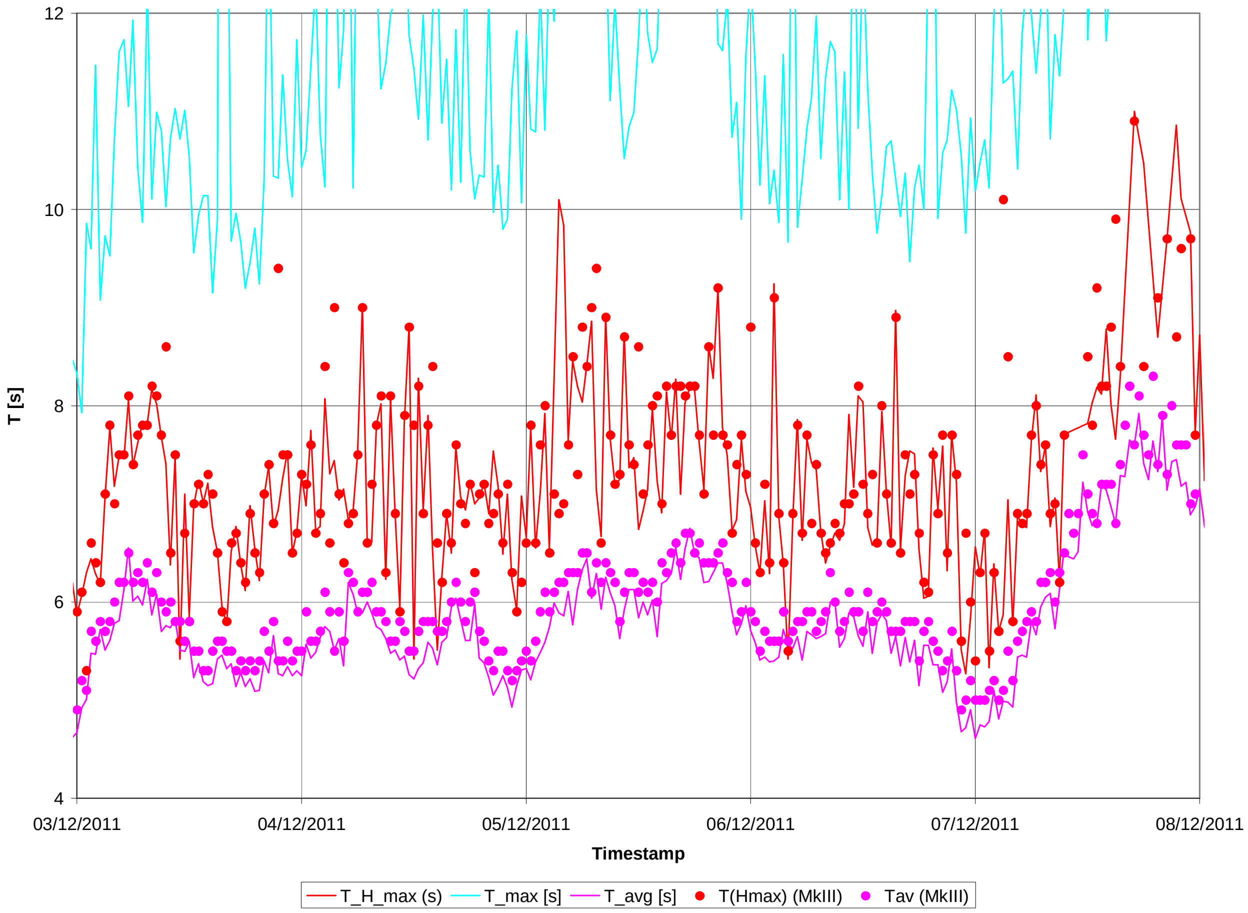


**Fig 7**. Wave period parameters in the zero-upcross wave analysis

From the higher sample rate and the higher resolution in the DWR4, this is actually not surprising. Near the mean sea level, the DWR4 has twice the number of datapoints, at ten times the resolution of the MkIII: where one scheme finds a zero-upcrossing, the other may not. The former buoy will report two short waves, the latter buoy a single long wave. In Figure 7, this effect is seen in the $T(H_{max})$ curves: either the two schemes have virtually identical values, or they differ substantially: where they do, one of the schemes, almost always the DWR4, has an extra zero-upcrossing in the highest wave. But actually this is a surprisingly rare event, occurring two or three times a day. This low occurrence also explains why the difference in the average wave period (i.e. in the number of waves) between the schemes is so small.
We can investigate this phenomenon a little closer, by looking at the number of crests, $N_c$. Here the same effects of doubled sample rate and resolution play a role. However, the effects are much stronger here, as can be seen in Figure 8. The number of crests that the DWR4 finds is close on a hundred greater than the number of crests in the MkIII, an increase of circa 20%. As a result, the bandwidth parameter $\varepsilon$, derived from the quotient of the number of waves and the number of crests, displays a significant shift from around 0.65 to 0.8. The conclusion from this structural break must be that the bandwidth $\varepsilon$ greatly depends on the sample rate and resolution, and that it is hence a poorly determined physical quantity. If the DWR4 heave data are filtered by a low-pass filter and rounded to centimetre resolution, the bandwidth parameter resumes its MkIII value. The difference in $\varepsilon$ between the schemes is thus not related to any error in either of them, but to its dependence on the sample rate.

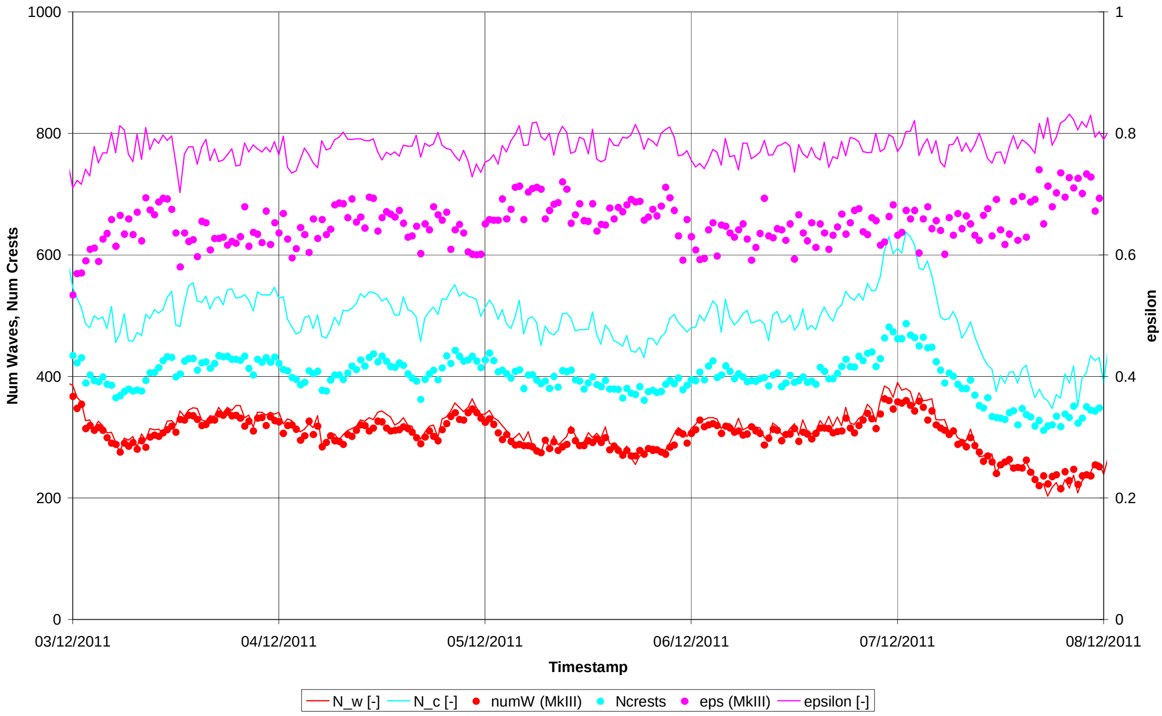


**Fig 8**. Number of waves $N_w$ and Number of crests $N_c$ (left axis) and bandwidth parameter $\varepsilon$ (eps, epsilon, right axis) in the zero-upcross wave analysis

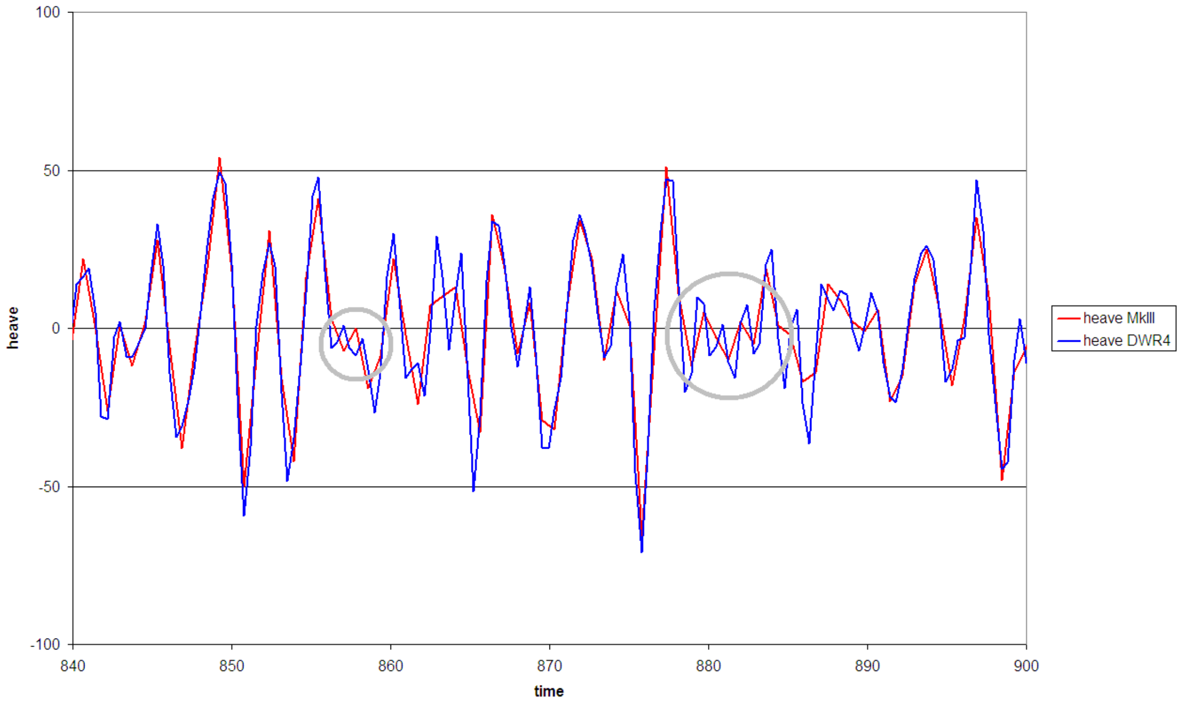


**Fig 9**. Detail of the heave time series of the MkIII (red solid line) and the DWR4 (blue solid line). The gray circles show regions where the DWR4 has extra crests (maxima).

An inspection of the heave time series of both buoy schemes in Figure 9 displays the same phenomenon in a direct way. In general, the series concur and the effect of the differences in sample rate and resolution remains invisible, apart from the DWR4 curve being somewhat smoother. At a few points in time, however, the extra information in the DWR4 yields an extra upcrossing or an extra crest. Two of these points are indicated by a gray circle. These minor differences lay at the basis of the trend break in the bandwidth parameter.

Please note that the spectral equivalent of $\varepsilon$, the spectral bandwidth parameter bearing the same name but determined from the crest period ($T_c$) and the zero-upcross period ($T_z$), suffers a similar problem. The fourth spectral moment, on which $T_c$ and hence $\varepsilon$ depend, is not finite for any current model spectrum (Pierson-Moskowitz, Bretschneider, JONSWAP), provided the integral is calculated on the full frequency interval from zero to infinity. In maths terms the integral is improper and divergent. Hence, theoretically $T_c$ equals zero and $\varepsilon$ is unity. In practice, the upper frequency will always be less than half the sampling frequency, and the now proper integral converges under all conditions. As a result, we do have nonzero crest periods and bandwidth values below unity. What we see in the zero-upcross bandwidth is the counterpart of this spectral phenomenon.
The conclusion from all this is that the bandwidth parameter, whether spectral or statistical, is not a good quantity to use in the scheme comparison. Its value depends crucially on measurement settings like the upper frequency limit, directly proportional to the sampling frequency, and the heave resolution. The inevitable structural break in this parameter is explainable and not indicative of any errors in either scheme.
In general, however, the conclusion from the wave-statistical results is no other than the conclusion from the spectral results: there is excellent concordance between both buoy schemes, even for parameters like the maximum wave height $H_{max}$ and the corresponding wave period $T(H_{max})$. Again, this positive result for the high-level parameters is implicit evidence for an agreement on all the low-level measurements involved.

## Individual heave spectra

Until now we investigated the high-level spectral and wave-statistical parameters, that summarize 30 minutes records into a single number. Let us now focus on individual, low-level results like the heave spectrum (in this section), and the directional spectrum (in the next section). More subtle differences or agreements not preserved by the global parameters may surface in the original 30 minutes records.
In Figure 10, a representative heave spectrum, pertaining to 1 December 2011, 22:30, is plotted. For the MkIII, the spectrum closest in time is that of 22:56, where this label refers to the time when the transmission from buoy to shore started. The heave data that it is based on dates from 22:26 to 22:53. The timestamps of the MkIII spectra are not synchronized to any real-world clock. In contrast, the timing of the DWR4 spectra is governed by the GPS clock in the buoy and matches the full and half hours of Coordinated Universal Time (UTC, without the leap seconds). Furthermore, the timestamps in the DWR4 refer to the start of the heave record that the spectrum is based on. Thus the heave data of the 22:30 spectrum is from 22:30 to 23:00, since the DWR4 spectrum spans the full 1800 seconds (and not just 1600 seconds as does the MkIII). The overlap between the two data sets is thus large, but not 100%.
The MkIII spectrum contains 64 frequency bins, between 0.025 and 0.58 Hz. The DWR4 spectrum has 100 frequency bins, between 0.025 and 1.0 Hz. In fact, the MkIII bins form a subset of the DWR4 bins, and by simply confining oneself to this subset, one can easily turn a DWR4 spectrum in a MkIII lookalike.
The extra bins of the DWR4 are not just at the high-frequency end of the spectrum. In the mid-range, 0.1 to 0.25 Hz, where the MkIII has a frequency spacing of 0.01 Hz, the DWR4 has a spacing of only 0.005 Hz, and this accounts for 15 additional bins. These extra mid-range bins are clearly discernible in Figure 10: the DWR4, in red, shows a few peaks and dips that the MkIII, in blue, does not, always at the frequencies where the DWR4 has a bin and the MkIII has not. Outside this interval, the match between the schemes' results is virtually perfect.
The gain at the high frequency end may not be immediately evident from the linear plot of the spectrum. The logarithmic plot of Figure 11 however shows a clear continuation of the $f^{-4}$ decline up to 0.8 Hz. Beyond this frequency, the hydrodynamic response of the buoy, being 70 cm in diameter, falls off rapidly. It would take a buoy diameter as small as

40 cm to utilize the full interval up to 1.0 Hz. This justifies the choice for 1.0 Hz as a frequency upper limit that serves the full range of Datawell buoy diameters.

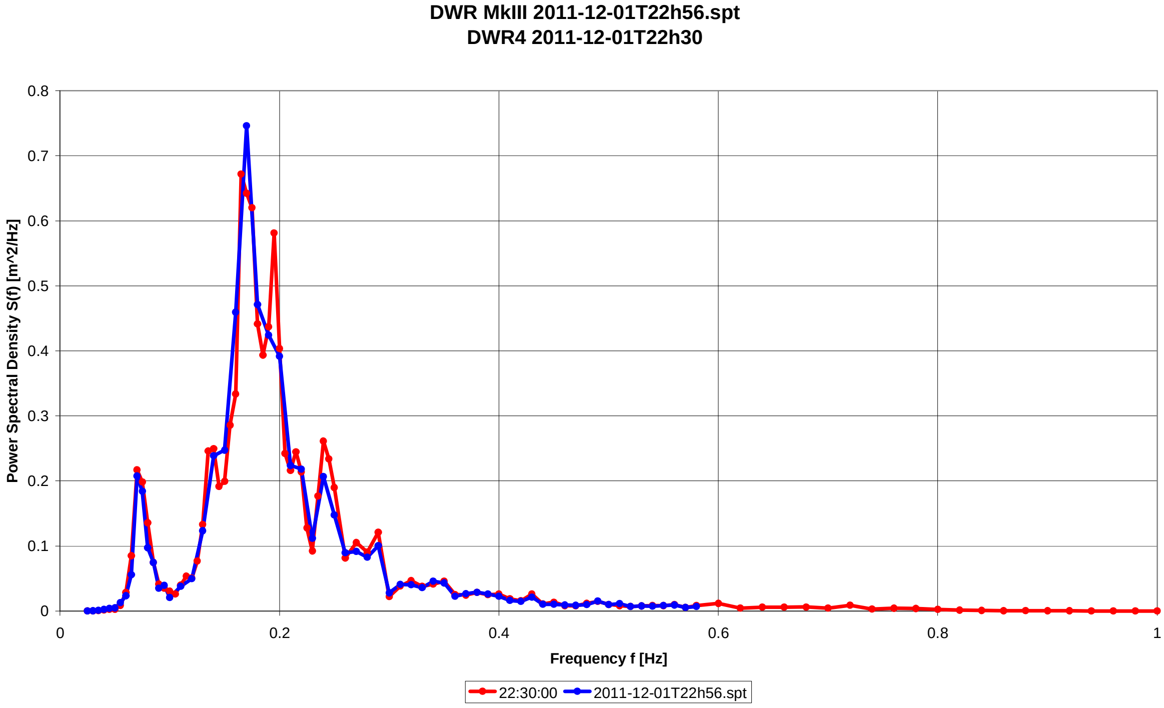


**Fig 10**. Heave spectrum of 1 December 2011, 22:30, for the DWR4 (red) and the MkIII (blue)

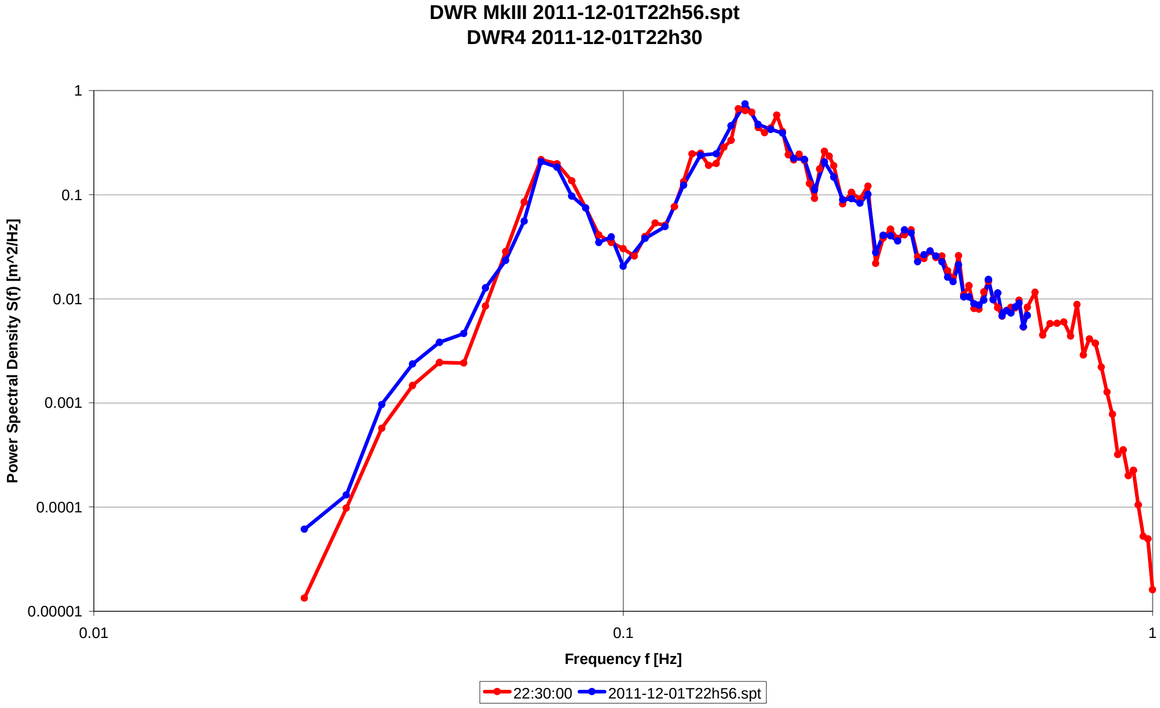


**Fig 11**. Logarithmic plot of the spectrum of Figure 10.

In conclusion, the heave spectra of both schemes display an excellent match, and they are much closer than any confidence interval guarantees. The extra mid-range bins in the DWR4 reveal some fine-structure of the spectrum, the high-frequency bins help determine the characteristics of the spectral fall-off here. The particular spectrum and the results discussed above are typical for all of the test period.

## Individual directional spectra

For the displacement data of the previous section we have investigated the directional spectrum as well. The directional parameters that are compared are those proposed by Kuik, Van Vledder and Holthuijsen, J Phys Ocean 18, 1988, p.1020, viz. the mean direction, the directional spread, the skewness and the kurtosis. These parameters suit well directional distributions that are unimodal. If one wave field is dominant, unimodality is a valid assumption and the directional spread is then a measure of the single peak's width. When more than one wave field is present, the spread is a measure of the angular distance between the peaks, rather than of the width of any peak.
In the present spectrum, the wave fields are manifest at different frequencies. A swell is seen around 0.075 Hz, coming from NNW. See Figure 12. The wind sea from 0.14 Hz is westerly. The DWR4 nicely coincides with the MkIII, reproducing even small details at frequencies with low energy. The MkIII curve ends at a northerly direction, suggesting that the wind is turning from W to N. This suggestion is corroborated by the extra bins of the DWR4. Beyond 0.8 Hz however the directional data is no longer considered reliable, in the light of the large buoy diameter.
The directional spread at the peaks' frequencies is quite small, some 20° to 30°, indicative of separate wave fields and unimodal directional distributions. Again, the two schemes agree nicely on trend and details. The results bring out the excellent quality of both the MkIII and the DWR4, or actually of the heave and direction sensors whose measurements underlie both schemes.
In Figure 13, the skewness and the kurtosis of the directional distribution are plotted. These parameters are less known. They depend on the third and fourth statistical moment, respectively, which are less well determinable.
The skewness is a measure of the asymmetry of the distribution. Qualitatively, a positive skewness indicates that the tail on the right side is longer than the left side and the bulk of the values lie to the left of the mean. Vice versa for negative skewness. To know what left and right mean in a circular distribution, one must realize that wave direction is direction from where the waves arrive, and that +90° corresponds to East. A northerly swell is skew positive if the tail of the distribution is towards the east.
In the figure the skewness (the lower curves, left axis) is seen to vary mainly between -2 and +2. Below 0.17 Hz the skewness has a negative dip, whereas above this frequency the skewness is slightly positive on average. Both schemes agree on this general trend, but the agreement on the details is much poorer.


Datawell BV
Zomerluststraat 4
2012 LM Haarlem
The Netherlands

T +31 23 531 60 53
F +31 23 531 19 86
E sales@datawell.nl
W www.datawell.nl

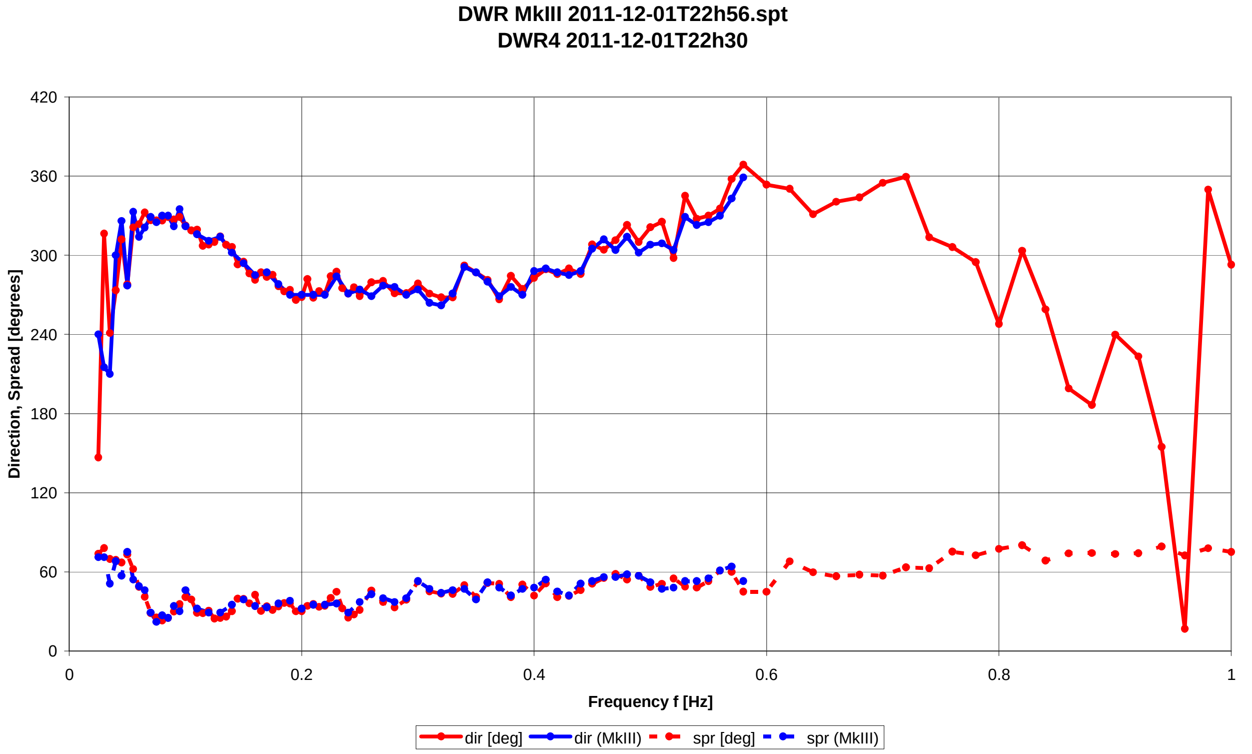


**Fig 12**. Mean direction and directional spread for the spectrum of Figure 10.

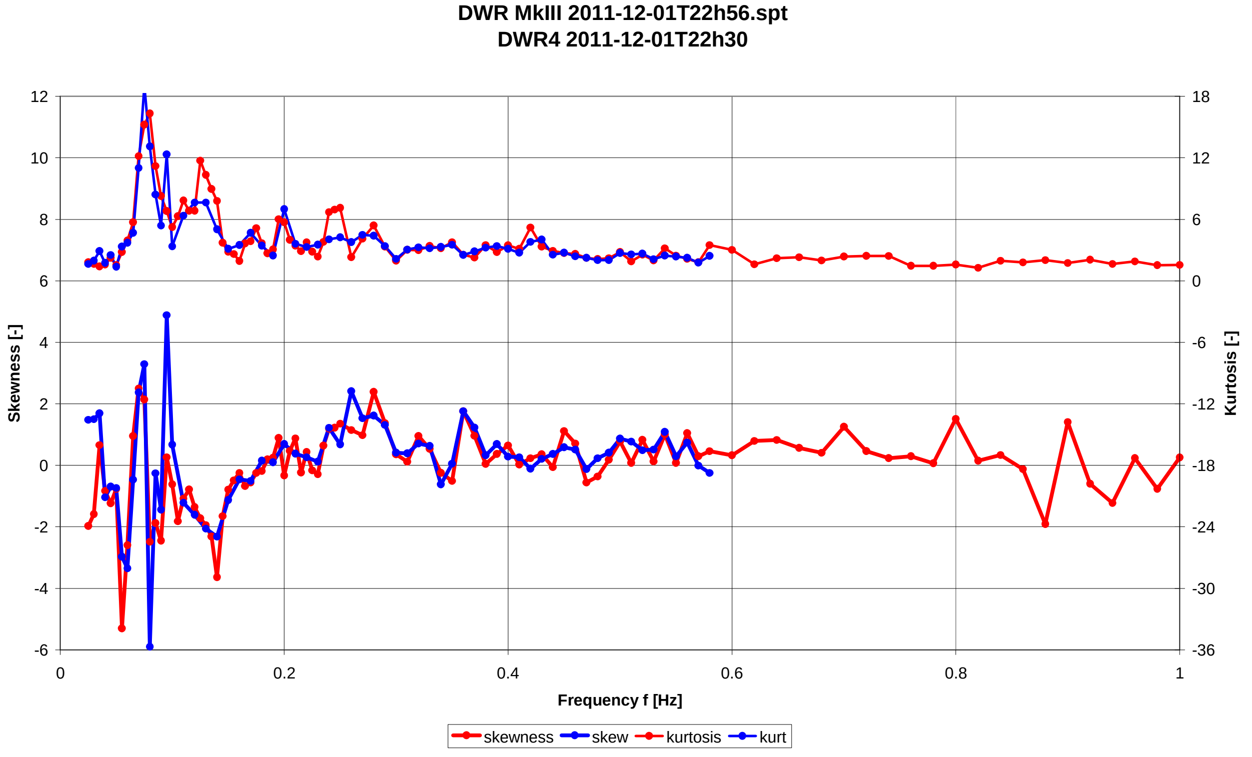


**Fig 13**. Skewness and Kurtosis for the spectrum of Figure 10.

Similar remarks apply to the kurtosis (the upper curves in Figure 13, right axis), which is a measure of the peakedness of the distribution. A large kurtosis corresponds to a distribution having a sharp peak. Small values of the kurtosis indicate a “broad” shape. The normal distribution has a kurtosis of 3. We see that the low-frequency swell has a kurtosis of almost 18, which suggests that its peak is quite acute. At the high-frequency end the kurtosis values are Gaussian or sub-Gaussian. Here too, the MkIII and the DWR4 agree on the general trend, but display quite a few incongruities when it comes to the details. Because the skewness and the kurtosis are essentially normalized higher moments, their values also depend on the directional spread that is used for the normalization.
In conclusion, the mean direction and directional spread for the two buoy schemes are in excellent agreement. The skewness and the kurtosis for the MkIII and the DWR4 show more variation. This variation however seems to be related to the nature of these secondary parameters that are less well-determined than the primary direction and spread.

## General conclusion

The introduction of the DWR4 has opened new possibilities in the analysis of wave data: higher sampling rate and improved resolution, more segments, better window functions yield more datapoints, more spectral bins, and a higher upper frequency limit. Excellent agreement on the main spectral and statistical parameters between the schemes prove that both the MkIII and the DWR4 are valid schemes of data analysis, and it corroborates the status of the Waverider as the golden standard in the field of wave measurement.
At the same time, comparison of the two buoy schemes elucidates the dependence of many wave parameters on the upper frequency limit / the sample frequency, a dependence that was implicit as long as the sample rate remained constant. Now, with a second scheme present having a different sample rate, this dependence becomes visible as a structural break in the bandwidth parameter $\varepsilon$.
The doubled sample frequency, now 2.56 Hz, accommodates all Datawell buoys – directional and non-directional –, and employs their full orbit-following capacity. Since now the hydrodynamic response is the limiting factor for buoys of any diameter – 40, 70 or 90 cm –, there is no need to increase the sample frequency any further.
From the individual spectra, it is seen that the heave spectrum, the mean direction and the directional spread are measured with great accuracy and rendered correctly in both schemes. The variability of the secondary parameters skewness and kurtosis is seen to be greater, and is understood to be cause of minor differences in these parameters between the schemes.
The advantages of the DWR4 in the field of computation and processing, besides its extensibility with new measurement options, will make it the obvious choice for measuring waves.